

STATIC DEFORMATIONS FROM POINT FORCES AND FORCE COUPLES LOCATED IN WELDED ELASTIC POISSONIAN HALF-SPACES: IMPLICATIONS FOR SEISMIC MOMENT TENSORS

BY THOMAS H. HEATON AND ROBERT E. HEATON

ABSTRACT

We present analytic expressions for the static deformations produced by point forces and point force couples embedded in two elastic Poissonian half-spaces that are welded on a horizontal interface. We show that the deformations from point forces and from vertically dipping strike-slip point double couples vary continuously (except at the strike-slip source) as the source is moved across the welded interface. We show that the pattern of deformations from vertically dipping (or horizontally dipping) dip-slip point double couples also vary continuously as the source is moved across the welded interface, but the amplitude of the deformations jumps by the ratio of the rigidities. Finally, we show that the pattern of deformation from a point explosion source or from a point double-couple source dipping at angles other than 0° or 90° jumps as the source is moved across the boundary. We demonstrate that integration of point double-couple sources on a plane of finite extent mimics the deformation of slip on a fault plane where the total moment of the double-couples is μAD . We also demonstrate that deformations from a distribution of double couples on a horizontally dipping finite plane just above the interface are indistinguishable from the deformations produced by a similar distribution of double couples located just below the interface but with a total moment that is different by the ratio of the rigidities. This demonstrates that the moment of a dislocation that occurs between two materials is ambiguously defined. We discuss reasons why seismic moment is not a very satisfying way to parameterize the size of an earthquake. We show that potency, defined to be the integral of the slip over the rupture surface, is a more natural size scaling parameter than seismic moment.

INTRODUCTION

The purpose of this paper is to derive and discuss the static deformation due to point force and force-couple systems in the vicinity of two welded, elastic Poissonian half-spaces. In particular, we are interested in the interpretation of seismic moment in the presence of heterogeneous media. For example, how does the elastic deformation change if a point double couple is moved from an infinitesimal distance above a boundary to an infinitesimal distance below a boundary? As we will show, the answer to this problem is somewhat complex and depends upon the orientation of the double couple with respect to the boundary. We will show that for a fixed moment, a vertical strike-slip double couple gives the same deformation throughout the media (except at the source point) regardless of whether it is infinitesimally above or below the interface. However, for a fixed moment, a vertical dip-slip double couple gives a deformation pattern that differs by the ratio, m , of the material rigidities depending on whether the source is above or below the interface. As has been previously noted by Woodhouse (1981) this can lead to ambiguities in the determination of the moment of earthquakes. We discuss why we believe that these ambiguities imply that seismic moment is not a very satisfying quantification of the size of an earthquake.

POINT-FORCE SOLUTIONS

Ben-Menahem and Gillon (1970) presented a technique for the computation of static deformations resulting from a point source embedded in an elastic layer bounded by a vacuum on top and an elastic half-space on the bottom. Sato (1971) and Sato and Matsu'ura (1973) extended these results to apply to any layered elastic space. However, the calculation of deformations using these solutions requires numerical integration techniques that might introduce ambiguities when limiting cases are investigated. Rongved (1955) derived Papkovitch functions (a type of displacement field potential, Fung, 1965) for an arbitrary point force within welded elastic half-spaces. Although the expressions for these potentials are closed-form algebraic expressions, they are also quite complex and Rongved did not present expressions for the resulting displacements, presumably because of the awkward length of the expressions that would result. However, Rongved's Papkovitch functions simplify significantly if the media are considered to be Poissonian (Poisson's ratio equal to $\frac{1}{4}$ or $\lambda = \mu$). Figure 1 sketches the cartesian coordinate frame chosen for this problem. The half-spaces are welded along the plane $z = 0$, a point force F_j in the j th direction is located at the point $(0, 0, c > 0)$ and the resulting displacement in the i th direction at the point (x, y, z) is denoted by $U_{i^j}(x, y, z \geq 0)$ and $U'_{i^j}(x, y, z \leq 0)$. The rigidities of the upper ($z > 0$) and lower ($z < 0$) half-spaces are μ and

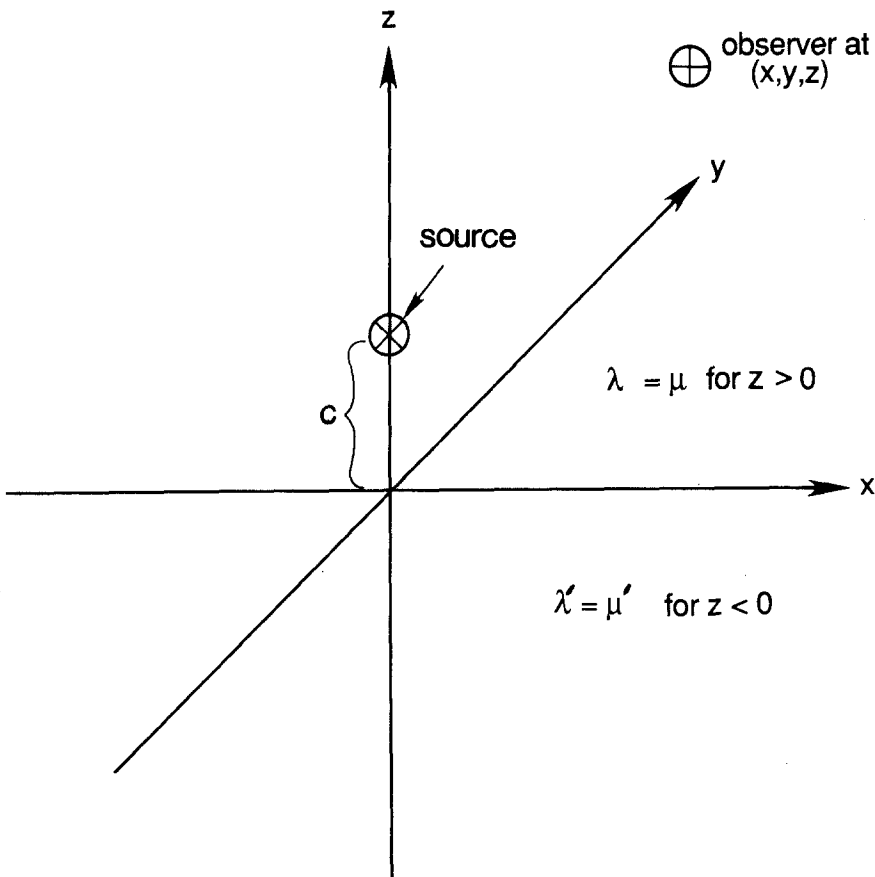


FIG. 1. Coordinate frame and source-observer geometry.

μ' , respectively. Following the notation of Rongved (1955), we define

$$m = \frac{\mu'}{\mu}, \tag{1}$$

$$R_1 = \sqrt{x^2 + y^2 + (z - c)^2}, \tag{2}$$

$$R_2 = \sqrt{x^2 + y^2 + (z + c)^2}. \tag{3}$$

For convenience, we also define

$$\mathfrak{R}_1 = R_1 - z + c, \tag{4}$$

$$\mathfrak{R}_2 = R_2 + z + c. \tag{5}$$

After some laborious algebraic manipulation of Rongved's (1955) solution, we find the following expressions for the displacements caused by a single point force.

$$\begin{aligned}
 U_x^x = & \frac{F_x}{12\pi\mu} \left[\frac{2}{R_1} + \frac{x^2}{R_1^3} \right] + \frac{(1-m)^2 F_x}{12\pi\mu(1+m)(2+m)(1+2m)} \left[\frac{1}{\mathfrak{R}_2} - \frac{x^2}{R_2 \mathfrak{R}_2^2} \right] \\
 & + \frac{(1-m)F_x}{12\pi\mu(1+m)(1+2m)} \\
 & \cdot \left[\frac{2(1+2m)}{R_2} + \frac{(1+2m)x^2 + 2(1+m)cz}{R_2^3} - \frac{6(1+m)czx^2}{R_2^5} \right] \\
 & + \frac{(1-m)(z+c)F_x}{12\pi\mu(1+m)(1+2m)} \left[\frac{-1}{R_2 \mathfrak{R}_2} + \frac{x^2}{R_2^3 \mathfrak{R}_2} + \frac{x^2}{R_2^2 \mathfrak{R}_2^2} \right], \tag{6}
 \end{aligned}$$

$$\begin{aligned}
 U'_{x^x} = & \frac{F_x}{6\pi\mu(1+m)} \left[\frac{2}{R_1} + \frac{x^2}{R_1^3} \right] \\
 & + \frac{(1-m)^2 F_x}{12\pi\mu(1+m)(2+m)(1+2m)} \left[\frac{1}{\mathfrak{R}_1} - \frac{x^2}{R_1 \mathfrak{R}_1^2} \right] \\
 & + \frac{(1-m)[(1+2m)z + (2+m)c]F_x}{12\pi\mu(1+m)(2+m)(1+2m)} \left[\frac{-1}{R_1 \mathfrak{R}_1} + \frac{x^2}{R_1^3 \mathfrak{R}_1} + \frac{x^2}{R_1^2 \mathfrak{R}_1^2} \right]. \tag{7}
 \end{aligned}$$

For U_y^y and U'_{y^y} , substitute y for x .

$$\begin{aligned}
 U_y^x = & \frac{xyF_x}{12\pi\mu R_1^3} + \frac{(1-m)xyF_x}{12\pi\mu(1+m)(1+2m)} \left[\frac{(1+2m)}{R_2^3} - \frac{6(1+m)cz}{R_2^5} \right] \\
 & - \frac{(1-m)^2 xyF_x}{12\pi\mu(1+m)(2+m)(1+2m)R_2 \mathfrak{R}_2^2} \\
 & + \frac{(1-m)(z+c)xyF_x}{12\pi\mu(1+m)(1+2m)} \left[\frac{1}{R_2^3 \mathfrak{R}_2} + \frac{1}{R_2^2 \mathfrak{R}_2^2} \right], \tag{8}
 \end{aligned}$$

$$U'_{y^x} = \frac{xyF_x}{6\pi\mu(1+m)R_1^3} - \frac{(1-m)^2xyF_x}{12\pi\mu(1+m)(2+m)(1+2m)R_1\mathfrak{R}_1^2} + \frac{(1-m)[(1+2m)z + (2+m)c]xyF_x}{12\pi\mu(1+m)(2+m)(1+2m)} \left[\frac{1}{R_1^3\mathfrak{R}_1} + \frac{1}{R_1^2\mathfrak{R}_1^2} \right]. \tag{9}$$

For U_x^y and U'_{x^y} , interchange x and y .

$$U_x^z = \frac{x(z-c)F_x}{12\pi\mu R_1^3} + \frac{(1-m)xF_x}{2\pi\mu(1+2m)} \left[\frac{z-c}{3R_2^3} - \frac{cz(z+c)}{R_2^5} \right] + \frac{(1-m)xF_x}{4\pi\mu(2+m)(1+2m)R_2\mathfrak{R}_2}, \tag{10}$$

$$U'_{z^x} = \frac{xF_x}{4\pi\mu(2+m)(1+2m)} \left[\frac{(1+2m)z - (2+m)c}{R_1^3} + \frac{(1-m)}{R_1\mathfrak{R}_1} \right]. \tag{11}$$

For U_z^y and U'_{z^y} , substitute y for x .

$$U_x^z = \frac{(z-c)xF_z}{12\pi\mu R_1^3} + \frac{(1-m)xF_z}{6\pi\mu(1+2m)} \left[\frac{z-c}{R_2^3} + \frac{3cz(z+c)}{R_2^5} \right] - \frac{(1-m)xF_z}{4\pi\mu(2+m)(1+2m)R_2\mathfrak{R}_2}, \tag{12}$$

$$U'_{x^z} = \frac{xF_z}{4\pi\mu(2+m)(1+2m)} \left[\frac{(1+2m)z - (2+m)c}{R_1^3} - \frac{1-m}{R_1\mathfrak{R}_1} \right]. \tag{13}$$

For U_y^z and U'_{y^z} , substitute y for x .

$$U_z^z = \frac{F_z}{6\pi\mu} \left[\frac{1}{R_1} + \frac{(z-c)^2}{2R_1^3} \right] + \frac{(1-m)F_z}{2\pi\mu(1+2m)} \cdot \left[\frac{4m+5}{6(2+m)R_2} + \frac{c(c+z)+z^2}{3R_2^3} + \frac{cz(z+c)^2}{R_2^5} \right] \tag{14}$$

$$U'_{z^z} = \frac{F_z}{4\pi\mu(2+m)(1+2m)} \left[\frac{3(1+m)}{R_1} + \frac{\{(1+2m)z - (2+m)c\}(z-c)}{R_1^3} \right]. \tag{15}$$

These solutions (6 through 15) only apply if the source is located in the unprimed half-space (i.e., $c > 0$). However, because of the symmetry about the plane $z = 0$, we can easily derive solutions for a source located in the primed half-space ($c < 0$) by an appropriate change of coordinates.

$$U_j^i(x, y, z \geq 0, c < 0, m, F_i) = -U'_j{}^i(-x, -y, -z, -c, 1/m, -F_i), \tag{16}$$

$$U'_j{}^i(x, y, z \leq 0, c < 0, m, F_i) = -U_j^i(-x, -y, -z, -c, 1/m, -F_i), \tag{17}$$

where the factor $1/m$ has the effect of interchanging μ and μ' everywhere in equations (6) through (15). That is, μ' should be explicitly substituted for μ , and $1/m$ should be substituted for m .

Notice that the expressions for the solution in the lower medium U_j^i involve powers of $1/R_1$, the distance from the source to the observer. However, the expressions for the solution in the upper medium U_j^i have both terms with powers of $1/R_1$ and terms with powers of $1/R_2$. R_2 is the distance to a virtual source located at a distance c beneath the interface.

RECIPROCAL RELATIONS

Although these solutions are fairly complex, it is a straightforward calculation to demonstrate the reciprocity relationships for point forces given by,

$$U_j^i(\mathbf{x}; \boldsymbol{\zeta}) = U_i^j(\boldsymbol{\zeta}; \mathbf{x}), \tag{18}$$

where \mathbf{x} and $\boldsymbol{\zeta}$ are the observer and source coordinates, respectively. The reciprocity theorem states that the solution is unchanged if the source and observer are interchanged. If the source and observer are both located in the unprimed half-space ($c > 0$ and $z > 0$), then the reciprocity equations for this problem can be written as

$$U_j^i(x, y, z, c, m) = U_i^j(-x, -y, c, z, m) \quad \text{if } z \geq 0, \tag{19}$$

If the observer is located in the primed half-space ($z < 0$), then the reciprocal source is located in the primed half-space and the solutions given by equation (16) must be used. For this particular problem, the reciprocity equations can be written as

$$U_j^i(x, y, z, c, m) = U_i^j(-x, -y, -c, -z, 1/m) \quad \text{if } z \leq 0. \tag{20}$$

In the expressions just given, the variables z and c should be interchanged and μ and μ' should be interchanged for expressions on the right-hand side of the equations.

POINT DOUBLE-COUPLE SOLUTIONS

For a point double-couple source with arbitrary orientation, the i th component of displacement, W_i , is given by

$$W_i = \sum_{j=1}^3 \sum_{k=1}^3 \xi_j \frac{M_{jk}}{F_{jk}} \frac{\partial U_i^j}{\partial x_k}, \tag{21}$$

where $x_1 = x$, $x_2 = y$, and $x_3 = c$; $\xi_1 = \xi_2 = 1$, $\xi_3 = -1$; and the moment tensor, M_{jk} , is given in BOX 4.4 of Aki and Richards (1980). The ξ_j terms are due to the fact that the partials should have been taken with respect to source coordinates and also because Aki and Richards (1980) define the positive z direction to be down. The partials of U_i^j with respect to x_k are given by the following expressions. Since spatial derivatives are taken with respect to the source coordinates, the forces F_j are

replaced by moments F_{jk} , where any c subscript is interchangeable with a z subscript.

$$\begin{aligned} \frac{\partial U_{xex}}{\partial x} &= \frac{-x^3 F_{xx}}{4\pi\mu R_1^5} \\ &+ \frac{(1-m)x F_{xx}}{4\pi\mu(1+m)(1+2m)} \left[-\frac{(1+2m)x^2 + 6(1+m)cz}{R_2^5} + \frac{10(1+m)cx^2 z}{R_2^7} \right] \\ &+ \frac{(1-m)^2 x F_{xx}}{12\pi\mu(1+m)(2+m)(1+2m)} \left[\frac{-3}{R_2^3 \mathfrak{R}_2^2} + \frac{x^2}{R_2^3 \mathfrak{R}_2^2} + \frac{2x^2}{R_2^2 \mathfrak{R}_2^3} \right] \\ &+ \frac{(1-m)(z+c)x F_{xx}}{4\pi\mu(1+m)(1+2m)} \left[\frac{1}{R_2^3 \mathfrak{R}_2} - \frac{x^2}{R_2^5 \mathfrak{R}_2} + \frac{1}{R_2^2 \mathfrak{R}_2^2} - \frac{x^2}{R_2^4 \mathfrak{R}_2^2} - \frac{2x^2}{3R_2^3 \mathfrak{R}_2^3} \right], \end{aligned} \tag{22}$$

$$\begin{aligned} \frac{\partial U'_{x^x}}{\partial x} &= \frac{-x^3 F_{xx}}{2\pi\mu(1+m)R_1^5} \\ &+ \frac{(1-m)^2 x F_{xx}}{12\pi\mu(1+m)(2+m)(1+2m)} \left[\frac{-3}{R_1^3 \mathfrak{R}_1^2} + \frac{x^2}{R_1^3 \mathfrak{R}_1^2} + \frac{2x^2}{R_1^2 \mathfrak{R}_1^3} \right] \\ &+ \frac{(1-m)\{(2+m)c + (1+2m)z\} x F_{xx}}{4\pi\mu(1+m)(2+m)(1+2m)} \\ &\cdot \left[\frac{1}{R_1^3 \mathfrak{R}_1} - \frac{x^2}{R_1^5 \mathfrak{R}_1} + \frac{1}{R_1^2 \mathfrak{R}_2^2} - \frac{x^2}{R_1^4 \mathfrak{R}_1^2} - \frac{2x^2}{3R_1^3 \mathfrak{R}_1^3} \right]. \end{aligned} \tag{23}$$

For $\frac{\partial U_y^y}{\partial y}$ and $\frac{\partial U'_{y^y}}{\partial y}$, substitute y for x .

$$\begin{aligned} \frac{\partial U_y^x}{\partial x} &= \frac{y F_{xx}}{12\pi\mu} \left[\frac{1}{R_1^3} - \frac{3x^2}{R_1^5} \right] \\ &+ \frac{(1-m)y F_{xx}}{12\pi\mu(1+m)(1+2m)} \\ &\cdot \left[\frac{(1+2m)}{R_2^3} - \frac{3(1+2m)x^2 + 6(1+m)cz}{R_2^5} + \frac{30(1+m)czx^2}{R_2^7} \right] \\ &+ \frac{(1-m)^2 y F_{xx}}{12\pi\mu(1+m)(2+m)(1+2m)} \left[\frac{-1}{R_2^3 \mathfrak{R}_2^2} + \frac{x^2}{R_2^3 \mathfrak{R}_2^2} + \frac{2x^2}{R_2^2 \mathfrak{R}_2^3} \right] \\ &+ \frac{(1-m)(z+c)y F_{xx}}{12\pi\mu(1+m)(1+2m)} \\ &\cdot \left[\frac{1}{R_2^3 \mathfrak{R}_2} - \frac{3x^2}{R_2^5 \mathfrak{R}_2} + \frac{1}{R_2^2 \mathfrak{R}_2^2} - \frac{3x^2}{R_2^4 \mathfrak{R}_2^2} - \frac{2x^2}{R_2^3 \mathfrak{R}_2^3} \right], \end{aligned} \tag{24}$$

$$\frac{\partial U'_{y^x}}{\partial x} = \frac{y F_{xx}}{6\pi\mu(1+m)} \left[\frac{1}{R_1^3} - \frac{3x^2}{R_1^5} \right]$$

$$\begin{aligned}
 & + \frac{(1-m)^2 y F_{xx}}{12\pi\mu(1+m)(2+m)(1+2m)} \left[\frac{-1}{R_1 \mathfrak{R}_1^2} + \frac{x^2}{R_1^3 \mathfrak{R}_1^2} + \frac{2x^2}{R_1^2 \mathfrak{R}_1^3} \right] \\
 & + \frac{(1-m)\{(1+2m)z + (2+m)c\} y F_{xx}}{12\pi\mu(1+m)(2+m)(1+2m)} \\
 & \cdot \left[\frac{1}{R_1^3 \mathfrak{R}_1} - \frac{3x^2}{R_1^5 \mathfrak{R}_1} + \frac{1}{R_1^2 \mathfrak{R}_1^2} - \frac{3x^2}{R_1^4 \mathfrak{R}_1^2} - \frac{2x^2}{R_1^3 \mathfrak{R}_1^3} \right]. \tag{25}
 \end{aligned}$$

For $\frac{\partial U_{x^y}}{\partial y}$ and $\frac{\partial U'_{x^y}}{\partial y}$, interchange x and y .

$$\begin{aligned}
 \frac{\partial U_z^x}{\partial x} & = \frac{(z-c)F_{xx}}{12\pi\mu} \left[\frac{1}{R_1^3} - \frac{3x^2}{R_1^5} \right] \\
 & + \frac{(1-m)F_{xx}}{4\pi\mu(2+m)(1+2m)} \left[\frac{1}{R_2 \mathfrak{R}_2} - \frac{x^2}{R_2^3 \mathfrak{R}_2} - \frac{x^2}{R_2^2 \mathfrak{R}_2^2} \right] \\
 & + \frac{(1-m)F_{xx}}{2\pi\mu(1+2m)} \left[\frac{z-c}{3R_2^3} - \frac{(z-c)x^2 + (c+z)cz}{R_2^5} + \frac{5(z+c)czx^2}{R_2^7} \right], \tag{26}
 \end{aligned}$$

$$\begin{aligned}
 \frac{\partial U'_z{}^x}{\partial x} & = \frac{F_{xx}}{4\pi\mu(2+m)(1+2m)} \\
 & \cdot \left[\frac{(1+2m)z - (2+m)c}{R_1^3} - \frac{3x^2\{(1+2m)z - (2+m)c\}}{R_1^5} \right] \\
 & + \frac{(1-m)F_{xx}}{4\pi\mu(2+m)(1+2m)} \left[\frac{1}{R_1 \mathfrak{R}_1} - \frac{x^2}{R_1^3 \mathfrak{R}_1} - \frac{x^2}{R_1^2 \mathfrak{R}_1^2} \right]. \tag{27}
 \end{aligned}$$

For $\frac{\partial U_{x^y}}{\partial y}$ and $\frac{\partial U'_z{}^y}{\partial y}$, substitute y for x .

$$\begin{aligned}
 \frac{\partial U_x^x}{\partial y} & = \frac{-yF_{xy}}{12\pi\mu} \left[\frac{2}{R_1^3} + \frac{3x^2}{R_1^5} \right] + \frac{(1-m)^2 y F_{xy}}{12\pi\mu(1+m)(2+m)(1+2m)} \\
 & \cdot \left[\frac{-1}{R_2 \mathfrak{R}_2^2} + \frac{x^2}{R_2^3 \mathfrak{R}_2^2} + \frac{2x^2}{R_2^2 \mathfrak{R}_2^3} \right] + \frac{(1-m)yF_{xy}}{12\pi\mu(1+m)(1+2m)} \\
 & \cdot \left[\frac{-2(1+2m)}{R_2^3} - \frac{3(1+2m)x^2 + 6(1+m)cz}{R_2^5} + \frac{30(1+m)czx^2}{R_2^7} \right] \\
 & + \frac{(1-m)(z+c)yF_{xy}}{12\pi\mu(1+m)(1+2m)} \left[\frac{1}{R_2^3 \mathfrak{R}_2} + \frac{1}{R_2^2 \mathfrak{R}_2^2} - \frac{3x^2}{R_2^5 \mathfrak{R}_2^2} - \frac{3x^2}{R_2^4 \mathfrak{R}_2^2} - \frac{2x^2}{R_2^3 \mathfrak{R}_2^3} \right], \tag{28}
 \end{aligned}$$

$$\frac{\partial U'_x{}^x}{\partial y} = \frac{-yF_{xy}}{6\pi\mu(1+m)} \left[\frac{2}{R_1^3} + \frac{3x^2}{R_1^5} \right]$$

$$\begin{aligned}
 & + \frac{(1-m)^2 y F_{xy}}{12\pi\mu(1+m)(2+m)(1+2m)} \left[\frac{-1}{R_1 \mathfrak{R}_1^2} + \frac{x^2}{R_1^3 \mathfrak{R}_1^2} + \frac{2x^2}{R_1^2 \mathfrak{R}_1^3} \right] \\
 & + \frac{(1-m)\{z(1+2m) + c(2+m)\} y F_{xy}}{12\pi\mu(1+m)(2+m)(1+2m)} \\
 & \cdot \left[\frac{1}{R_1^3 \mathfrak{R}_1} + \frac{1}{R_1^2 \mathfrak{R}_1^2} - \frac{3x^2}{R_1^5 \mathfrak{R}_1} - \frac{3x^2}{R_1^4 \mathfrak{R}_1^2} - \frac{2x^2}{R_1^3 \mathfrak{R}_1^3} \right].
 \end{aligned} \tag{29}$$

For $\frac{\partial U_y^y}{\partial x}$ and $\frac{\partial U'_y^y}{\partial x}$, interchange x and y .

$$\begin{aligned}
 \frac{\partial U_y^x}{\partial y} & = \frac{x F_{xy}}{12\pi\mu} \left[\frac{1}{R_1^3} - \frac{3y^2}{R_1^5} \right] \\
 & + \frac{(1-m)^2 x F_{xy}}{12\pi\mu(1+m)(2+m)(1+2m)} \left[\frac{y^2}{R_2^3 \mathfrak{R}_2^2} + \frac{2y^2}{R_2^2 \mathfrak{R}_2^3} \right] \\
 & + \frac{(1-m)x F_{xy}}{12\pi\mu(1+m)(1+2m)} \\
 & \cdot \left[\frac{(1+2m)}{R_2^3} - \frac{3(1+2m)y^2 + 6(1+m)cz}{R_2^5} + \frac{30(1+m)czy^2}{R_2^7} \right] \\
 & + \frac{(1-m)(z+c)x F_{xy}}{12\pi\mu(1+m)(1+2m)} \\
 & \cdot \left[\frac{1}{R_2^3 \mathfrak{R}_2} + \frac{1}{R_2^2 \mathfrak{R}_2^2} - \frac{3y^2}{R_2^5 R_2} - \frac{3y^2}{R_2^4 \mathfrak{R}_2^2} - \frac{2y^2}{R_2^3 \mathfrak{R}_2^3} \right],
 \end{aligned} \tag{30}$$

$$\begin{aligned}
 \frac{\partial U'_y^x}{\partial y} & = \frac{x F_{xy}}{6\pi\mu(1+m)} \left[\frac{1}{R_1^3} - \frac{3y^2}{R_1^5} \right] \\
 & + \frac{(1-m)^2 x F_{xy}}{12\pi\mu(1+m)(2+m)(1+2m)} \left[\frac{y^2}{R_1^3 \mathfrak{R}_1^2} + \frac{2y^2}{R_1^2 \mathfrak{R}_1^3} \right] \\
 & + \frac{(1-m)\{z(1+2m) + c(2+m)\} x F_{xy}}{12\pi\mu(1+m)(2+m)(1+2m)} \\
 & \cdot \left[\frac{1}{R_1^3 \mathfrak{R}_1} + \frac{1}{R_1^2 \mathfrak{R}_1^2} - \frac{3y^2}{R_1^5 \mathfrak{R}_1} - \frac{3y^2}{R_1^4 \mathfrak{R}_1^2} - \frac{2y^2}{R_1^3 \mathfrak{R}_1^3} \right].
 \end{aligned} \tag{31}$$

For $\frac{\partial U_x^y}{\partial x}$ and $\frac{\partial U'_x^y}{\partial x}$, interchange x and y .

$$\begin{aligned}
 \frac{\partial U_z^x}{\partial y} & = \frac{(c-z)xy F_{xy}}{4\pi\mu R_1^5} \\
 & - \frac{(1-m)xy F_{xy}}{2\pi\mu(1+2m)} \left[\frac{z-c}{R_2^5} - \frac{5cz(z+c)}{R_2^7} + \frac{1}{2(2+m)R_2^3 \mathfrak{R}_2} + \frac{1}{2(2+m)R_2^2 \mathfrak{R}_2^2} \right],
 \end{aligned} \tag{32}$$

$$\frac{\partial U'_z{}^x}{\partial y} = \frac{-xyF_{xy}}{4\pi\mu(2+m)(1+2m)} \left[\frac{-3(2+m)c + 3(1+2m)z}{R_1^5} + \frac{(1-m)}{R_1^3\mathfrak{R}_1} + \frac{(1-m)}{R_1^2\mathfrak{R}_1^2} \right]. \tag{33}$$

For $\frac{\partial U_z{}^y}{\partial x}$ and $\frac{\partial U'_z{}^y}{\partial x}$, interchange x and y .

$$\begin{aligned} \frac{\partial U_x{}^x}{\partial c} &= \frac{(z-c)F_{xz}}{12\pi\mu} \left[\frac{2}{R_1^3} + \frac{3x^2}{R_1^5} \right] \\ &+ \frac{(1-m)F_{xz}}{2\pi\mu(1+2m)} \left[\frac{-x^2(2z+c) - cz(z+c)}{R_2^5} + \frac{5(z+c)czx^2}{R_2^7} \right] \\ &+ \frac{(1-m)[(1-2m)z - (1+4m)c]F_{xz}}{12\pi\mu(1+m)(1+2m)R_2^3} \\ &+ \frac{(1-m)F_{xz}}{4\pi\mu(1+m)(2+m)(1+2m)} \left[\frac{-1}{R_2\mathfrak{R}_2} + \frac{x^2}{R_2^3\mathfrak{R}_2} + \frac{x^2}{R_2^2\mathfrak{R}_2^2} \right], \end{aligned} \tag{34}$$

$$\begin{aligned} \frac{\partial U'_x{}^x}{\partial c} &= \frac{[(1+2m)(m+3)z - (2+m)(1+3m)c]F_{xz}}{4\pi\mu(1+m)(2+m)(1+2m)R_1^3} \\ &+ \frac{3\{(1+2m)z - (2+m)c\}x^2F_{xz}}{4\pi\mu(2+m)(1+2m)R_1^5} \\ &+ \frac{(1-m)F_{xz}}{4\pi\mu(1+m)(2+m)(1+2m)} \left[\frac{-1}{R_1\mathfrak{R}_1} + \frac{x^2}{R_1^3\mathfrak{R}_1} + \frac{x^2}{R_1^2\mathfrak{R}_1^2} \right]. \end{aligned} \tag{35}$$

For $\frac{\partial U_y{}^y}{\partial c}$ and $\frac{\partial U'_y{}^y}{\partial c}$, substitute x for y .

$$\begin{aligned} \frac{\partial U_y{}^x}{\partial c} &= \frac{(z-c)xyF_{xz}}{4\pi\mu R_1^5} - \frac{(1-m)xyF_{xz}}{2\pi\mu(1+2m)} \left[\frac{2z+c}{R_2^5} - \frac{5(z+c)cz}{R_2^7} \right] \\ &+ \frac{(1-m)xyF_{xz}}{4\pi\mu(1+m)(2+m)(1+2m)} \left[\frac{1}{R_2^3\mathfrak{R}_2} + \frac{1}{R_2^2\mathfrak{R}_2^2} \right], \end{aligned} \tag{36}$$

$$\begin{aligned} \frac{\partial U'_y{}^x}{\partial c} &= \frac{3\{(1+2m)z - (2+m)c\}xyF_{xz}}{4\pi\mu(2+m)(1+2m)R_1^5} \\ &+ \frac{(1-m)xyF_{xz}}{4\pi\mu(1+m)(2+m)(1+2m)} \left[\frac{1}{R_1^3\mathfrak{R}_1} + \frac{1}{R_1^2\mathfrak{R}_1^2} \right]. \end{aligned} \tag{37}$$

For $\frac{\partial U_x^y}{\partial c}$ and $\frac{\partial U_x'^y}{\partial c}$, interchange x and y .

$$\begin{aligned} \frac{\partial U_z^x}{\partial c} &= \frac{x F_{xz}}{12\pi\mu} \left[\frac{-1}{R_1^3} + \frac{3(z-c)^2}{R_1^5} \right] \\ &\quad - \frac{(1-m)x F_{xz}}{12\pi\mu(1+2m)} \left[\frac{2m+7}{(2+m)R_2^3} + \frac{12(z+c)z - 6c^2}{R_2^5} - \frac{30(z+c)^2 cz}{R_2^7} \right], \end{aligned} \tag{38}$$

$$\frac{\partial U_z'^x}{\partial c} = \frac{3x F_{xz}}{4\pi\mu(2+m)(1+2m)} \left[\frac{-1}{R_1^3} + \frac{\{(1+2m)z - (2+m)c\}(z-c)}{R_1^5} \right]. \tag{39}$$

For $\frac{\partial U_z^y}{\partial c}$ and $\frac{\partial U_z'^y}{\partial c}$, substitute y for x .

$$\begin{aligned} \frac{\partial U_x^y}{\partial x} &= \frac{(z-c)F_{zx}}{12\pi\mu} \left[\frac{1}{R_1^3} - \frac{3x^2}{R_1^5} \right] + \frac{(1-m)(z-c)F_{zx}}{6\pi\mu(1+2m)R_2^3} \\ &\quad + \frac{(1-m)F_{zx}}{2\pi\mu(1+2m)} \left[\frac{(z+c)cz - (z-c)x^2}{R_2^5} - \frac{5(z+c)czx^2}{R_2^7} \right] \\ &\quad + \frac{(1-m)F_{zx}}{4\pi\mu(2+m)(1+2m)} \left[\frac{-1}{R_2\mathfrak{R}_2} + \frac{x^2}{R_2^3\mathfrak{R}_2} + \frac{x^2}{R_2^2\mathfrak{R}_2^2} \right], \end{aligned} \tag{40}$$

$$\begin{aligned} \frac{\partial U_x'^z}{\partial x} &= \frac{\{(1+2m)z - (2+m)c\}F_{zx}}{4\pi\mu(2+m)(1+2m)R_1^3} - \frac{3\{(1+2m)z - (2+m)c\}x^2 F_{zx}}{4\pi\mu(2+m)(1+2m)R_1^5} \\ &\quad + \frac{(1-m)F_{zx}}{4\pi\mu(2+m)(1+2m)} \left[\frac{-1}{R_1\mathfrak{R}_1} + \frac{x^2}{R_1^3\mathfrak{R}_1} + \frac{x^2}{R_1^2\mathfrak{R}_1^2} \right]. \end{aligned} \tag{41}$$

For $\frac{\partial U_y^z}{\partial y}$ and $\frac{\partial U_y'^z}{\partial y}$, substitute x for y .

$$\begin{aligned} \frac{\partial U_y^z}{\partial x} &= \frac{(c-z)xy F_{zx}}{4\pi\mu R_1^5} - \frac{(1-m)xy F_{zx}}{2\pi\mu(1+2m)} \left[\frac{z-c}{R_2^5} + \frac{5(z+c)cz}{R_2^7} \right] \\ &\quad + \frac{(1-m)xy F_{zx}}{4\pi\mu(2+m)(1+2m)} \left[\frac{1}{R_2^3\mathfrak{R}_2} + \frac{1}{R_2^2\mathfrak{R}_2^2} \right], \end{aligned} \tag{42}$$

$$\begin{aligned} \frac{\partial U_y'^z}{\partial x} &= \frac{3\{(2+m)c - (1+2m)z\}xy F_{zx}}{4\pi\mu(2+m)(1+2m)R_1^5} \\ &\quad + \frac{(1-m)xy F_{zx}}{4\pi\mu(2+m)(1+2m)} \left[\frac{1}{R_1^3\mathfrak{R}_1} + \frac{1}{R_1^2\mathfrak{R}_1^2} \right]. \end{aligned} \tag{43}$$

For $\frac{\partial U_x^z}{\partial y}$ and $\frac{\partial U_x'^z}{\partial y}$, interchange x and y .

$$\begin{aligned} \frac{\partial U_z^z}{\partial x} &= \frac{-xF_{zx}}{12\pi\mu} \left[\frac{2}{R_1^3} + \frac{3(z-c)^2}{R_1^5} \right] \\ &\quad - \frac{(1-m)x F_{zx}}{12\pi\mu(1+2m)} \left[\frac{4m+5}{(2+m)R_2^3} + \frac{6(c^2+cz+z^2)}{R_2^5} + \frac{30(z+c)^2 cz}{R_2^7} \right], \end{aligned} \tag{44}$$

$$\frac{\partial U_z'^z}{\partial x} = \frac{-3xF_{zx}}{4\pi\mu(2+m)(1+2m)} \left[\frac{1+m}{R_1^3} + \frac{\{(1+2m)z - (2+m)c\}(z-c)}{R_1^5} \right]. \tag{45}$$

For $\frac{\partial U_z^z}{\partial y}$ and $\frac{\partial U_z'^z}{\partial y}$, substitute y for x .

$$\begin{aligned} \frac{\partial U_x^z}{\partial c} &= \frac{x F_{zz}}{12\pi\mu} \left[\frac{-1}{R_1^3} + \frac{3(z-c)^2}{R_1^5} \right] \\ &\quad + \frac{(1-m)x F_{zz}}{6\pi\mu(1+2m)} \left[\frac{-(1+2m)}{2(2+m)R_2^3} + \frac{6cz+3c^2}{R_2^5} - \frac{15cz(z+c)^2}{R_2^7} \right], \end{aligned} \tag{46}$$

$$\frac{\partial U_x'^z}{\partial c} = \frac{-x F_{zz}}{4\pi\mu(2+m)R_1^3} + \frac{3\{(1+2m)z - (2+m)c\}(z-c)x F_{zz}}{4\pi\mu(2+m)(1+2m)R_1^5}. \tag{47}$$

For $\frac{\partial U_y^z}{\partial c}$ and $\frac{\partial U_y'^z}{\partial c}$, substitute y for x .

$$\begin{aligned} \frac{\partial U_z^z}{\partial c} &= \frac{(z-c)^3 F_{zz}}{4\pi\mu R_1^5} \\ &\quad + \frac{(1-m)F_{zz}}{2\pi\mu(1+2m)} \left[\frac{3c - (1+2m)z}{6(2+m)R_2^3} + \frac{c(2z-c)(z+c)}{R_2^5} - \frac{5cz(z+c)^3}{R_2^7} \right], \end{aligned} \tag{48}$$

$$\frac{\partial U_z'^z}{\partial c} = \frac{(1-m)c F_{zz}}{4\pi\mu(2+m)(1+2m)R_1^3} + \frac{3\{(1+2m)z - (2+m)c\}(z-c)^2 F_{zz}}{4\pi\mu(2+m)(1+2m)R_1^5}. \tag{49}$$

The following identities were particularly useful in the derivation of these formulas.

$$\frac{f(x, y, z)(z+c)^n}{R_2^i \mathfrak{R}_2^j} + \frac{f(x, y, z)(z+c)^{n-1}}{R_2^{i-1} \mathfrak{R}_2^j} = \frac{f(x, y, z)(z+c)^{n-1}}{R_2^i \mathfrak{R}_2^{j-1}}, \tag{50}$$

$$\frac{f(x, y, z)(z-c)^n}{R_1^i \mathfrak{R}_1^j} - \frac{f(x, y, z)(z-c)^{n-1}}{R_1^{i-1} \mathfrak{R}_1^j} = -\frac{f(x, y, z)(z-c)^{n-1}}{R_1^i \mathfrak{R}_1^{j-1}}. \tag{51}$$

$$\frac{\partial R_i}{\partial x_j} = \frac{x_j}{R_i}, \quad \text{for } i = 1 \text{ or } 2, \text{ and } j = 1 \text{ or } 2. \tag{52}$$

$$\frac{\partial R_1}{\partial z} = \frac{(z - c)}{R_1} = -\frac{\partial R_1}{\partial c}, \quad \frac{\partial R_2}{\partial z} = \frac{(z + c)}{R_2} = \frac{\partial R_2}{\partial c}, \tag{53}$$

$$\frac{\partial \left(\frac{1}{R_1 \mathfrak{R}_1} \right)}{\partial z} = \frac{1}{R_1^3} = -\frac{\partial \left(\frac{1}{R_1 \mathfrak{R}_1} \right)}{\partial c}, \tag{54}$$

$$\frac{\partial \left(\frac{1}{R_2 \mathfrak{R}_2} \right)}{\partial z} = -\frac{1}{R_2^3} = \frac{\partial \left(\frac{1}{R_2 \mathfrak{R}_2} \right)}{\partial c}. \tag{55}$$

If the source is located in the primed half-space ($c < 0$), then symmetry about the plane $z = 0$ can be used to show that

$$\frac{\partial U_j^i(x, y, z \geq 0, c < 0, m, F_i)}{\partial x_k} = -\frac{\partial U_j^i(-x, -y, -z, -c, 1/m, F_i)}{\partial x_k}, \tag{56}$$

$$\frac{\partial U_j^i(x, y, z \leq 0, c < 0, m, F_i)}{\partial x_k} = -\frac{\partial U_j^i(-x, -y, -z, -c, 1/m, F_i)}{\partial x_k}, \tag{57}$$

where the factor $1/m$ has the effect of interchanging μ and μ' everywhere in equations (22) through (49).

It is possible to demonstrate that the solutions for point double couples (given by W_i in equation 21) converge to whole-space solutions (which can be derived simply by setting $m = 1$) in the limit as R_1 approaches 0 for any $c > 0$. This is a nice demonstration of the fact that the seismic moment of an equivalent point dislocation depends only on the rigidity of its immediate surroundings (see equation 3.5 of Aki and Richards, 1980).

BEHAVIOR AT THE INTERFACE

We now investigate the nature of these solutions as the source is moved across the welded boundary at $z = 0$. If

$$U_j^i(x, y, z, c = 0^+) = U_j^i(x, y, z, c = 0^-), \tag{58}$$

then the solution for point forces is continuous as the source is moved across the welded boundary. Equations (16) and (58) can be combined to rewrite this condition as

$$U_j^i(x, y, z, c = 0, m) = U_j^i(-x, -y, -z, c = 0, 1/m). \tag{59}$$

It is straightforward to verify that equation (59) is true for all i and j . However, the situation is more complex for double-couple solutions. Let us consider the two cases of a vertical strike-slip double couple ($M_{12} = M_{21} = 1$, all other $M_{jk} = 0$) and a

vertical dip-slip double couple ($M_{13} = M_{31} = 1$, all other $M_{jk} = 0$). First consider a vertical strike-slip double couple.

$$W_i^{ss} = \frac{\partial U_i^x}{\partial y} + \frac{\partial U_i^y}{\partial x}, \tag{60}$$

or

$$\begin{aligned} W_x^{ss} = & \frac{M_0 y}{12\pi\mu} \left[\frac{-1}{R_1^3} - \frac{6x^2}{R_1^5} \right] + \frac{(1-m)^2 y M_0}{12\pi\mu(1+m)(2+m)(1+2m)} \\ & \cdot \left[\frac{-1}{R_2^2 \mathfrak{R}_2^2} + \frac{2x^2}{R_2^3 \mathfrak{R}_2^2} + \frac{4x^2}{R_2^2 \mathfrak{R}_2^3} \right] + \frac{(1-m)y M_0}{12\pi\mu(1+m)(1+2m)} \\ & \cdot \left[\frac{-(1+2m)}{R_2^3} - \frac{6(1+2m)x^2 + 12(1+m)cz}{R_2^5} + \frac{60(1+m)czx^2}{R_2^7} \right] \\ & + \frac{(1-m)(z+c)y M_0}{6\pi\mu(1+m)(1+2m)} \left[\frac{1}{R_2^3 \mathfrak{R}_2} + \frac{1}{R_2^2 \mathfrak{R}_2^2} - \frac{3x^2}{R_2^5 \mathfrak{R}_2} - \frac{3x^2}{R_2^4 \mathfrak{R}_2^2} - \frac{2x^2}{R_2^3 \mathfrak{R}_2^3} \right]. \end{aligned} \tag{61}$$

For W_y^{ss} , interchange x and y .

$$\begin{aligned} W_z^{ss} = & \frac{(c-z)xy M_0}{2\pi\mu R_1^5} - \frac{(1-m)xy M_0}{\pi\mu(1+2m)} \left[\frac{z-c}{R_2^5} - \frac{5cz(z+c)}{R_2^7} \right. \\ & \left. + \frac{1}{2(2+m)R_2^3 \mathfrak{R}_2} + \frac{1}{2(2+m)R_2^2 \mathfrak{R}_2^2} \right] \end{aligned} \tag{62}$$

$$\begin{aligned} W'_x{}^{ss} = & \frac{-y M_0}{6\pi\mu(1+m)} \left[\frac{1}{R_1^3} + \frac{6x^2}{R_1^5} \right] \\ & + \frac{(1-m)^2 y M_0}{12\pi\mu(1+m)(2+m)(1+2m)} \left[\frac{-1}{R_1 \mathfrak{R}_1^2} + \frac{2x^2}{R_1^3 \mathfrak{R}_1^2} + \frac{4x^2}{R_1^2 \mathfrak{R}_1^3} \right] \\ & + \frac{[(z+2c) + m(c+2z)](1-m)y M_0}{6\pi\mu(1+m)(2+m)(1+2m)} \\ & \cdot \left[\frac{1}{R_1^3 \mathfrak{R}_1} + \frac{1}{R_1^2 \mathfrak{R}_1^2} - \frac{3x^2}{R_1^5 \mathfrak{R}_1} - \frac{3x^2}{R_1^4 \mathfrak{R}_1^2} - \frac{2x^2}{R_1^3 \mathfrak{R}_1^3} \right]. \end{aligned} \tag{63}$$

For $W'_y{}^{ss}$, interchange x and y .

$$W'_z{}^{ss} = \frac{-3xy M_0}{2\pi\mu(2+m)(1+2m)} \left[\frac{z-2c+m(2z-c)}{R_1^5} + \frac{1-m}{3R_1^3 \mathfrak{R}_1} + \frac{1-m}{3R_1^2 \mathfrak{R}_1^2} \right]. \tag{64}$$

As was the case in equation (59), we can demonstrate that the solution for a vertical strike-slip double couple is continuous as the source moves across the welded boundary by showing that

$$W_i^{ss}(x, y, z, c = 0, m) = -W_i'^{ss}(-x, -y, -z, c = 0, 1/m), \quad (65)$$

a fact that can be verified by direct substitution, which yields

$$\begin{aligned} W_x^{ss}(x, y, z, c = 0, m) &= -W'_x{}^{ss}(-x, -y, -z, c = 0, 1/m) = \frac{-yM_0}{6\pi\mu(1+m)} \left[\frac{1}{R^3} + \frac{6x^2}{R^5} \right] \\ &+ \frac{(1-m)yzM_0}{6\pi\mu(1+m)(1+2m)} \\ &\cdot \left[\frac{1}{R^3(R+z)} + \frac{1}{R^2(R+z)^2} - \frac{3x^2}{R^5(R+z)} - \frac{3x^2}{R^4(R+z)^2} - \frac{2x^2}{R^3(R+z)^3} \right] \\ &+ \frac{(1-m)^2yM_0}{12\pi\mu(1+m)(2+m)(1+2m)} \\ &\cdot \left[\frac{-1}{R(R+z)^2} + \frac{2x^2}{R^3(R+z)^2} + \frac{4x^2}{R^2(R+z)^3} \right]. \end{aligned} \quad (66)$$

For W_y^{ss} and $W'_y{}^{ss}$, interchange x and y .

$$\begin{aligned} W_z^{ss}(x, y, z, c = 0, m) &= -W'_z{}^{ss}(-x, -y, -z, c = 0, 1/m) \\ &= \frac{-3xyzM_0}{2\pi\mu(1+2m)R^5} - \frac{(1-m)xyM_0}{2\pi\mu(2+m)(1+2m)} \left[\frac{1}{R^3(R+z)} + \frac{1}{R^2(R+z)^2} \right], \end{aligned} \quad (67)$$

where

$$R = \sqrt{x^2 + y^2 + z^2}. \quad (68)$$

Some care must be taken with the expressions above since they are only true if $R > 0$. If we first take the limit as $R_1 \rightarrow 0$ and then as $c \rightarrow 0$, we find that the solution at the point source does jump as we cross the boundary. This is consistent with the fact that the moments for identical point dislocations just above and below the boundary differ by the factor m .

In the case of a vertical dip-slip double couple we find that

$$W_i^{ds} = \frac{\partial U_i^z}{\partial x} - \frac{\partial U_i^x}{\partial c}, \quad (69)$$

or

$$\begin{aligned} W_x^{ds} &= \frac{(z-c)M_0}{12\pi\mu} \left[\frac{1}{R_1^3} + \frac{6x^2}{R_1^5} \right] - \frac{(1-m)[(1+4m)z - (1-2m)c]M_0}{12\pi\mu(1+m)(1+2m)R_2^3} \\ &- \frac{(1-m)M_0}{2\pi\mu(1+2m)} \left[\frac{2cz(z+c) + (2c+z)x^2}{R_2^5} - \frac{10(z+c)czx^2}{R_2^7} \right] \end{aligned}$$

$$+ \frac{m(1-m)M_0}{4\pi\mu(1+m)(2+m)(1+2m)} \left[\frac{1}{R_2\mathfrak{R}_2} - \frac{x^2}{R_2^3\mathfrak{R}_2} - \frac{x^2}{R_2^2\mathfrak{R}_2^2} \right], \tag{70}$$

$$W_y^{ds} = \frac{(z-c)xyM_0}{2\pi\mu R_1^5} + \frac{(1-m)xyM_0}{2\pi\mu(1+2m)} \left[\frac{-(z+2c)}{R_2^5} + \frac{10(z+c)cz}{R_2^7} \right] \\ - \frac{m(1-m)xyM_0}{4\pi\mu(1+m)(2+m)(1+2m)} \left[\frac{1}{R_2^3\mathfrak{R}_2} + \frac{1}{R_2^2\mathfrak{R}_2^2} \right], \tag{71}$$

$$W_z^{ds} = \frac{xM_0}{12\pi\mu} \left[\frac{1}{R_1^3} + \frac{6(z-c)^2}{R_1^5} \right] \\ - \frac{(1-m)xM_0}{6\pi\mu(1+2m)} \left[\frac{1-m}{(m+2)R_2^3} - \frac{3(z^2-2c^2+cz)}{R_2^5} + \frac{30cz(z+c)^2}{R_2^7} \right], \tag{72}$$

$$W'_{x \ dx} = \frac{[(1+2m)z - m(2+m)c]M_0}{2\pi\mu(1+m)(2+m)(1+2m)R_1^3} + \frac{3x^2[(1+2m)z - (2+m)c]M_0}{2\pi\mu(2+m)(1+2m)R_1^5} \\ - \frac{m(1-m)M_0}{4\pi\mu(1+m)(2+m)(1+2m)} \left[\frac{-1}{R_1\mathfrak{R}_1} + \frac{x^2}{R_1^3\mathfrak{R}_1} + \frac{x^2}{R_1^2\mathfrak{R}_1^2} \right], \tag{73}$$

$$W'_{y \ ds} = \frac{3[(1+2m)z - (2+m)c]xyM_0}{2\pi\mu(2+m)(1+2m)R_1^5} \\ - \frac{m(1-m)xyM_0}{4\pi\mu(1+m)(2+m)(1+2m)} \left[\frac{1}{R_1^3\mathfrak{R}_1} + \frac{1}{R_1^2\mathfrak{R}_1^2} \right], \tag{74}$$

$$W'_{z \ ds} = \frac{3xM_0}{4\pi\mu(2+m)(1+2m)} \left[\frac{m}{R_1^3} + \frac{2\{(1+2m)z - (2+m)c\}(z-c)}{R_1^5} \right]. \tag{75}$$

We can demonstrate that the solution for a vertical dip-slip double couple is not continuous as the source moves across the welded boundary by showing that

$$W_i^{ds}(x, y, z, c = 0, m) \neq -W'_i{}^{ds}(-x, -y, -z, c = 0, 1/m), \tag{76}$$

$$W_x^{ds}(x, y, z, c = 0, m) = \frac{m^2zM_0}{2\pi\mu(1+m)(1+2m)R^3} + \frac{m3xz^2M_0}{2\pi\mu(1+2m)R^5} \\ + \frac{m(1-m)M_0}{4\pi\mu(1+m)(1+2m)(2+m)} \left[\frac{1}{R(R+z)} - \frac{x^2}{R^3(R+z)} - \frac{x^2}{R^2(R+z)^2} \right], \tag{77}$$

$$W'_{x \ ds}(-x, -y, -z, c = 0, 1/m) = -\frac{mzM_0}{2\pi\mu(1+m)(2+m)R^3} - \frac{3x^2zM_0}{2\pi\mu(1+2m)R^5}$$

$$-\frac{(1-m)M_0}{4\pi\mu(1+m)(1+2m)(2+m)}\left[\frac{1}{R(R+z)}-\frac{x^2}{R^3(R+z)}-\frac{x^2}{R^2(R+z)^2}\right], \quad (78)$$

$$W_y^{ds}(x, y, z, c=0, m) = \frac{m3xyzM_0}{2\pi\mu(1+2m)R^5} \\ - \frac{m(1-m)xyM_0}{4\pi\mu(1+m)(1+2m)(2+m)}\left[\frac{1}{R^3(R+z)}+\frac{1}{R^2(R+z)^2}\right], \quad (79)$$

$$W_y'^{ds}(-x, -y, -z, c=0, 1/m) = -\frac{3xyzM_0}{2\pi\mu(1+2m)R^5} \\ + \frac{(1-m)xyM_0}{4\pi\mu(1+m)(1+2m)(2+m)}\left[\frac{1}{R^3(R+z)}+\frac{1}{R^2(R+z)^2}\right], \quad (80)$$

$$W_z^{ds}(x, y, z, c=0, m) = \frac{m3xM_0}{4\pi\mu(2+m)(1+2m)R^3} + \frac{m3xz^2M_0}{2\pi\mu(1+2m)R^5}, \quad (81)$$

$$W_z'^{ds}(-x, -y, -z, c=0, 1/m) = -\frac{3xM_0}{4\pi\mu(2+m)(1+2m)R^3} - \frac{3xz^2M_0}{2\pi\mu(1+2m)R^5}. \quad (82)$$

We see that all of the terms in the solutions for a vertical dip-slip double couple located just above the boundary differ from those for a source just below the boundary by the ratio of the rigidities m . The stress and strain boundary conditions are the ultimate cause of the difference in the way that the solutions for strike-slip and dip-slip double couples behave at the welded boundary. The predominant strain component in the strike-slip case (ϵ_{xy}) is continuous across the boundary, whereas the predominant strain component in the dip-slip case (ϵ_{xz}) is not continuous across the boundary. However, since the stress τ_{xz} is continuous across the boundary, and since shear stress and strain are simply related by the rigidity, the solutions for the dip-slip case vary by the ratio of the rigidities as the source is moved across the boundary.

If we consider a vertically dipping point double couple of an arbitrary rake, then we could obtain identical solutions, $W_i^+ = W_i(x, y, z, c=0^+)$, everywhere (except at the source point) for a source with a rake angle λ^+ located just above the boundary and for a source with a different rake angle λ^- located just below the boundary. λ^+ and λ^- are related by the following expression.

$$W_i^{+ss} \cos(\lambda^+) + W_i^{+ds} \sin(\lambda^+) = W_i^{+ss} \cos(\lambda^-) + \frac{W_i^{+ds} \sin(\lambda^-)}{m}. \quad (83)$$

Thus if one knew the deformations (except at the source) produced by a vertically dipping point double couple located in the vicinity of a boundary, then the rake angle could not be deduced unless it was known whether the source was located slightly above or slightly below the boundary.

The diagonal elements of the moment tensor (M_{ii}) are nonzero for solutions involving arbitrarily dipping point double couples or for point explosions. For the case of a horizontally oriented compressive point force couple, the solution varies continuously as the source is moved across the boundary since

$$\begin{aligned} \frac{\partial U_x^x(x, y, z, c = 0, m)}{\partial x} &= -\frac{\partial U_x^x(-x, -y, -z, c = 0, 1/m)}{\partial x} = \frac{-x^3 F_{xx}}{2\pi\mu(1+m)R^5} \\ &+ \frac{(1-m)^2 x F_{xx}}{12\pi\mu(1+m)(2+m)(1+2m)} \\ &\cdot \left[\frac{-3}{R^3 \mathfrak{R}^2} + \frac{x^2}{R^3 \mathfrak{R}^2} + \frac{2x^2}{R^2 \mathfrak{R}^3} \right] \\ &+ \frac{(1-m)zx F_{xx}}{4\pi\mu(1+m)(1+2m)} \\ &\cdot \left[\frac{1}{R^3 \mathfrak{R}} - \frac{x^2}{R^5 \mathfrak{R}} + \frac{1}{R^2 \mathfrak{R}^2} - \frac{x^2}{R^4 \mathfrak{R}^2} - \frac{2x^2}{3R^3 \mathfrak{R}^3} \right], \end{aligned} \tag{84}$$

$$\begin{aligned} \frac{\partial U_y^x(x, y, z, c = 0, m)}{\partial x} &= -\frac{\partial U_y^x(-x, -y, -z, c = 0, 1/m)}{\partial x} = \frac{y F_{xx}}{6\pi\mu(1+m)} \left[\frac{1}{R^3} - \frac{3x^2}{R^5} \right] \\ &+ \frac{(1-m)^2 y F_{xx}}{12\pi\mu(1+m)(2+m)(1+2m)} \\ &\cdot \left[\frac{-1}{R^3 \mathfrak{R}^2} + \frac{x^2}{R^3 \mathfrak{R}^2} + \frac{2x^2}{R^2 \mathfrak{R}^3} \right] + \frac{(1-m)zy F_{xx}}{12\pi\mu(1+m)(1+2m)} \\ &\cdot \left[\frac{1}{R^3 \mathfrak{R}} - \frac{3x^2}{R^5 \mathfrak{R}} + \frac{1}{R^2 \mathfrak{R}^2} - \frac{3x^2}{R^4 \mathfrak{R}^2} - \frac{2x^2}{R^3 \mathfrak{R}^3} \right], \end{aligned} \tag{85}$$

$$\begin{aligned} \frac{\partial U_z^x(x, y, z, c = 0, m)}{\partial x} &= -\frac{\partial U_z^x(-x, -y, -z, c = 0, 1/m)}{\partial x} = \frac{z F_{xx}}{4\pi\mu(1+2m)} \left[\frac{1}{R^3} - \frac{3x^2}{R^5} \right] \\ &+ \frac{(1-m)F_{xx}}{4\pi\mu(2+m)(1+2m)} \left[\frac{1}{R \mathfrak{R}} - \frac{x^2}{R^3 \mathfrak{R}} - \frac{x^2}{R^2 \mathfrak{R}^2} \right]. \end{aligned} \tag{86}$$

The displacements produced by a vertically oriented point force couple are discontinuous and vary in the following complex way as the source is moved across the boundary.

$$\frac{\partial U_x^z(x, y, z, c = 0, m)}{\partial c} = \frac{-x F_{zz}}{4\pi\mu(2+m)R^3} + \frac{z^2 x F_{zz}}{4\pi\mu R^5}, \tag{87}$$

$$\frac{\partial U_x^z(-x, -y, -z, c = 0, 1/m)}{\partial c} = \frac{-x F_{zz}}{4\pi\mu(1+2m)R^3} + \frac{3z^2 x F_{zz}}{4\pi\mu(1+2m)R^5}, \tag{88}$$

$$\frac{\partial U_z^z(x, y, z, c = 0, m)}{\partial c} = \frac{-(1 - m)zF_{zz}}{12\pi\mu(2 + m)R^3} + \frac{z^3F_{zz}}{4\pi\mu R^5}, \quad (89)$$

$$-\frac{\partial U_z^z(-x, -y, -z, c = 0, 1/m)}{\partial c} = \frac{3z^3F_{zz}}{4\pi\mu(1 + 2m)R^5}. \quad (90)$$

In this case, we see that not only does the amplitude of the displacements change as the source is moved across the boundary, but their spatial pattern changes also. If one attempted to invert data to find the nature of a point source located on one side of a boundary that matched displacements produced by a source on the opposite side of the boundary, then spurious conclusions could result. For instance, one might find that a source with a non-double-couple component may better fit displacements that were produced by a purely double-couple source located on the other side of the boundary. Similar ambiguities can be found in the solutions for far-field waves radiated by point moment-tensor sources (Woodhouse, 1981).

NUMERICAL EXAMPLES

In order to explore the nature of these solutions further, we have constructed a computer code that calculates displacements, strains, and stresses on any two-dimensional plane cutting through the four-dimensional space (x, y, z, c). Strains are calculated by numerical differentiation of the solution with respect to observer coordinates and the stresses are calculated from the strains in the usual way. These numerical solutions also allow us to verify that the displacements and appropriate strains and stresses are continuous across the welded boundary. In Figures 2 and 3 we show contours of displacements, strains, and stresses that result from a vertical dip-slip point double couple ($M_0 = 10^{25}$ dyne-cm) striking parallel to the x axis and located 1 km above the boundary between two half-spaces having rigidities of 10^{11} and 2×10^{11} dyne-cm $^{-2}$. The y coordinate of the observer is fixed at 2 km and the x and z coordinates both vary from -2 km to $+2$ km. As is expected from the boundary conditions at $z = 0$, we see that $U_x, U_z, \epsilon_{xx}, \tau_{xz}$, and τ_{zz} are all continuous at $z = 0$ (as are U_y, ϵ_{yy} , and τ_{yz} which are not shown) and $\epsilon_{xz}, \epsilon_{zz}$, and τ_{xx} are discontinuous at $z = 0$ (as are ϵ_{yz} and τ_{yy} , which are not shown). We prepared similar plots for all of the point-force and point-force-couple solutions given in this paper to verify that the solutions satisfy the required boundary conditions.

In order to investigate the behavior of these solutions as a point source is moved across the welded interface, we show contour plots of displacement for observers with x coordinates that vary from -2 km to $+2$ km (horizontal axis of contour plot) and source locations that vary from -2 km to $+2$ km (vertical axis of contour plot). The y coordinate of the observers is fixed at 2 km and the z coordinate is fixed at 1 km. The rigidities of the upper and lower media are 10^{11} and 2×10^{11} dyne-cm $^{-2}$, respectively. In Figure 4, we show contours of the resulting x and z components of displacement for both a vertical strike-slip double couple and a vertical dip-slip double couple. The couples strike parallel to the x axis and the moment is assumed to be 10^{25} dyne-cm. It is clear from these figures that the solution for the vertical strike-slip double couple varies continuously as the source is moved across the boundary (see also equations 66 and 67), whereas the solution for the vertical dip-slip double-couple jumps by the ratio of the rigidities as the source moves across the boundary (see also equations 77 to 82). The situation is even more complex when other fault orientations are chosen. We show contours of the displacements

Vertical Dip-Slip Double-Couple

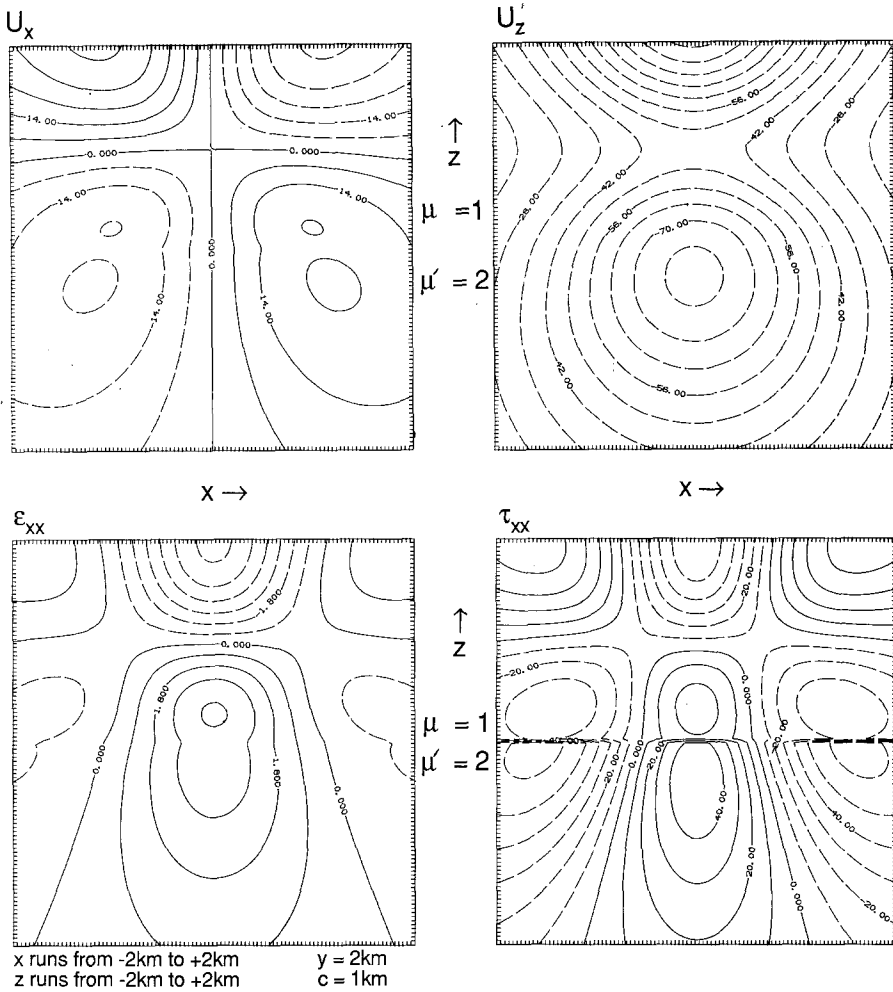


FIG. 2. Deformations from a vertically dipping point dip-slip double couple, striking parallel to the x axis and located 1 km above a material interface at $z = 0$. Deformations are contoured on a vertical plane parallel to the double couple ($y = 2$ km), where x and z both vary from -2 km to $+2$ km. The rigidities of the upper and lower media are 10^{11} and 2×10^{11} dyne-cm $^{-2}$, respectively. Displacements are given in cm, strains in 10^{-4} , stresses in bars, and the moment is 10^{25} dyne-cm. U_x , U_z , and ϵ_{xx} are continuous at the interface and τ_{xx} is discontinuous at the interface.

produced by 45° -dipping strike-slip and dip-slip double couples as a function of x and c in Figure 5. We see that not only does the amplitude jump, but the entire pattern of the deformation changes as the source crosses the interface (see also equations 87 through 90).

In Figure 6, we show similar contour plots for compressive force couples directed along both the x axis ($M_{xx} = 10^{25}$ dyne-cm) and the z -axis ($M_{zz} = 10^{25}$ dyne-cm). We see that the displacements produced by horizontally oriented compressive force couples vary continuously as the source is moved across the boundary (see also equations 85 to 86), whereas the displacements (and also the pattern of deformation) produced by a vertically oriented compressive force couple jump as the source is moved across the boundary (see also equations 87 to 90). In Figure 7, we show

Vertical Dip-Slip Double-Couple

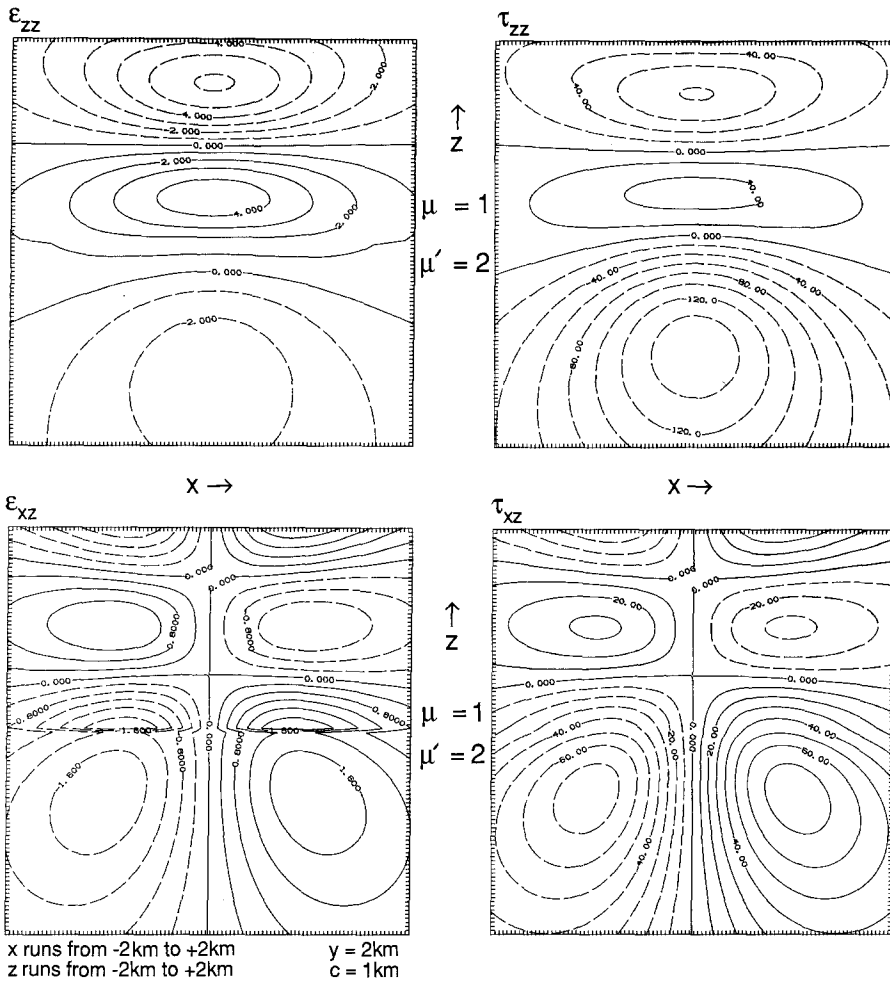


FIG. 3. Continuation of Figure 2, the same parameters are used but different components of the deformation are shown. τ_{zz} and τ_{xz} are continuous at the interface and ϵ_{zz} and ϵ_{xz} are discontinuous.

similar contour plots for point explosion sources ($M_{xx} = M_{yy} = M_{zz} = 10^{25}$ dyne-cm) and for point single-force sources ($F_x = F_y = F_z = 10^{13}$ dyne). Displacements produced by the explosion source jump as the source crosses the interface, and the displacements produced by point forces of any orientation vary continuously as the source crosses the interface (see also equation 59).

FINITE-FAULT NUMERICAL EXAMPLES

Up to this point we have confined our discussion to point force systems. Haskell (1964) showed that a dislocation D on a vanishingly small fault plane of area A results in solutions identical to that of an appropriately oriented point double-couple force system with a moment $M_0 = \mu AD$. We would like to investigate the relationship between dislocations on fault planes and equivalent force systems when the source is located near a material boundary. However, these solutions are singular at the source point and it is difficult to investigate the behavior of our solutions in the immediate vicinity of the source. The displacements produced by dislocations

Point Double Couples as They Cross a Boundary

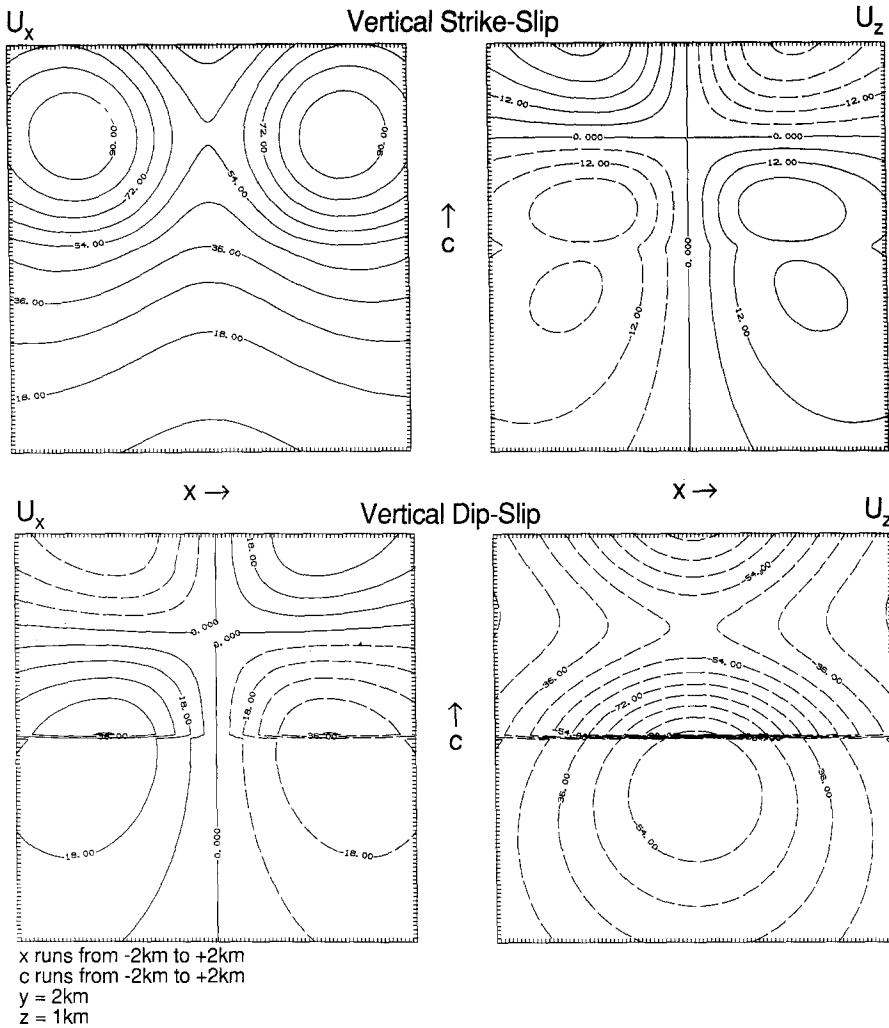


FIG. 4. Displacements from vertically dipping point strike-slip (upper panels) and dip-slip (lower panels) double couples striking parallel to the x axis. The x coordinate of the observer varies from -2 km to $+2$ km along the horizontal axis of the contour plots and the height of the source above the interface (the variable c) varies from -2 km to $+2$ km along the vertical axis of the contour plots. The y and z coordinates of the observer are fixed at 2 km and 1 km, respectively. The rigidities of the upper and lower media are 10^{11} and 2×10^{11} dyne-cm $^{-2}$, respectively. The sources both have moments of 10^{25} dyne-cm and the displacements are given in cm. Notice that the displacements from a vertical strike-slip double couple vary continuously as the source crosses the interface at $c = 0$, but the displacements from a vertical dip-slip double couple jump in amplitude by a factor of 2 (the ratio of the rigidities) as the source crosses the interface.

on faults of finite area are nonsingular and it is much easier to visualize the behavior of the solution in the immediate vicinity of the source. The solution for a dislocation on a finite fault can be obtained by integrating the appropriate point double-couple force over the area of a fault plane. Mansinha and Smylie (1971) have performed this integration analytically for the case of a finite fault embedded within an elastic half-space in contact with a vacuum. Although analytic integration of the double-couple solutions embedded within welded elastic half-spaces should be straightforward, it would also be exceedingly tedious.

Point Double-Couples as They Cross a Boundary

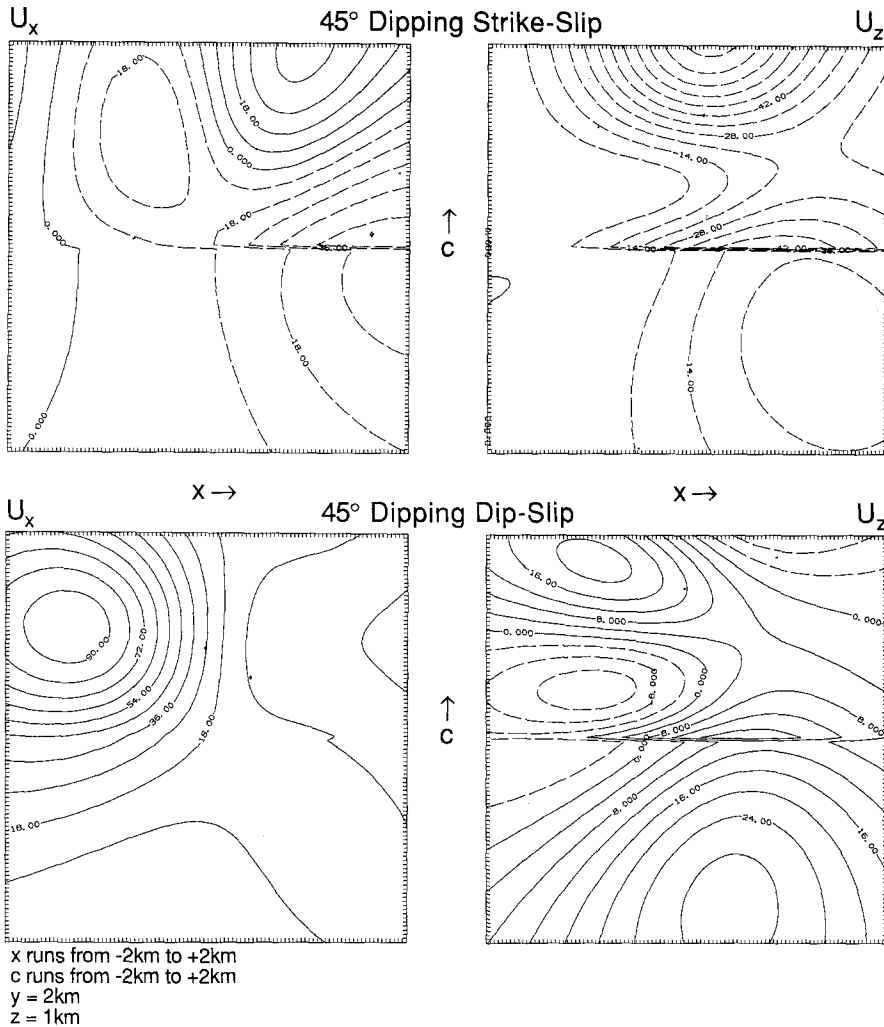


FIG. 5. Same as Figure 4, but for 45°-dipping strike-slip double couples (upper panels) and 45°-dipping dip-slip double couples. The double couples strike parallel to the x axis. Notice that in both cases, the pattern of displacements jumps as the source crosses the interface at $c = 0$. The components of a moment tensor for a point source lying on one side of the interface resulting from the inversion of data produced by a source lying on the opposite side of the interface would result in incorrect conclusions about the source orientation and may also result in spurious non-double-couple components from the inversion.

We have numerically integrated double-couple solutions over the fault plane by summing the response of many small finite subfaults whose individual response is approximated by point double-couples located in the center of each subfault. In Figure 8, we show the displacement parallel to the slip direction for a vertical strike-slip fault and a vertical dip-slip fault. The fault is actually the summation of a gridwork of 100 point double-couples running along the x axis from -2 km to $+2$ km by 100 point double-couples running along the z axis from -2 km to $+2$ km. The moment (10^{25} dyne-cm) is evenly distributed on the fault plane and the rigidity is 1.0×10^{11} and 2.0×10^{11} dyne/cm² for the upper and lower media, respectively.

Point Compressive Couples as They Cross a Boundary

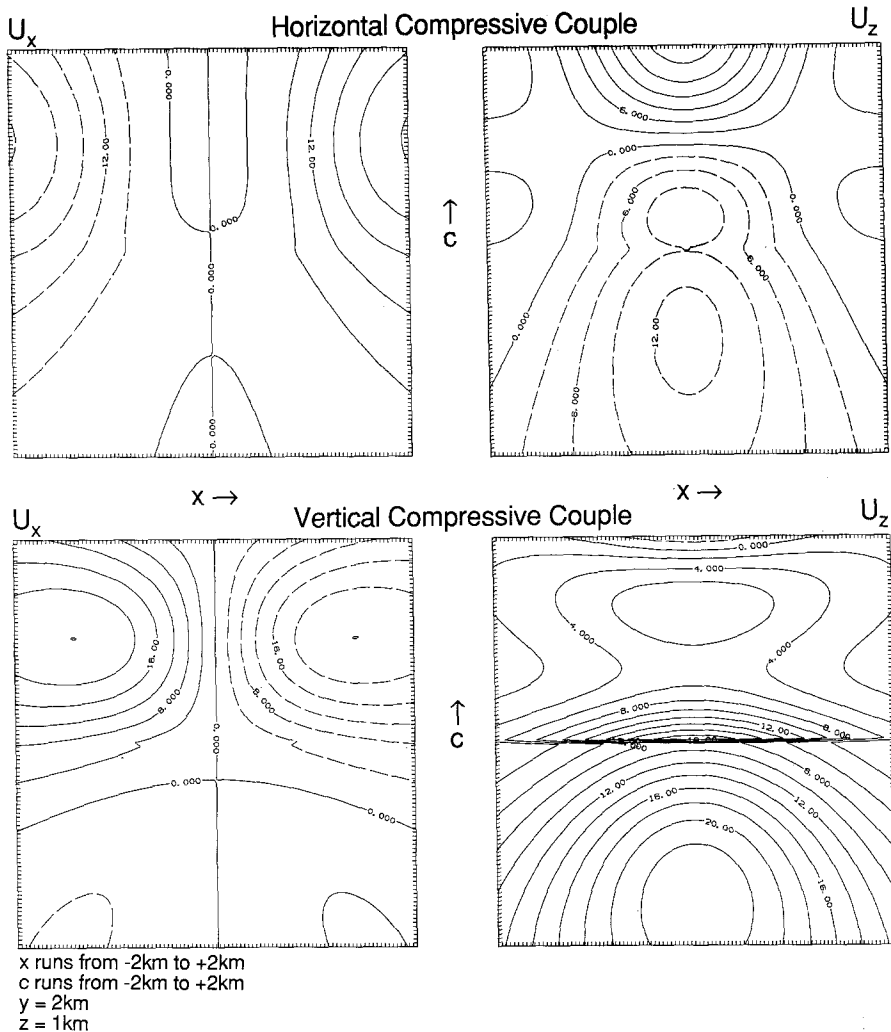


FIG. 6. Same as Figure 4, but for horizontal single compressive couples (upper panels) and vertical single compressive couples. Notice that the deformation from the horizontal compressive couple varies continuously as the source crosses the interface, but the pattern of the deformation from the vertical compressive-couple jumps as the source crosses the interface.

In panels 8a and 8c, the observer points are located on a gridwork that is parallel to that of the fault and located just 0.06 km from the fault; $y = 0.06$ km, 30 points run along the x axis from -3 km to $+3$ km and 30 points run along the z axis from -3 km to $+3$ km. In panels 8b and 8d, the observer points are located on a gridwork that is perpendicular to the fault plane; $x = 0$, y runs from -3 km to $+3$ km, and z runs from -3 km to $+3$ km.

It is readily apparent that these distributions on point double couples produce a deformation that mimics a dislocation on a fault plane. As expected, the amplitude of the dislocation is inversely proportional to the rigidity of the surrounding media: $D = M_0/\mu A$. Although the displacements produced by a vertical strike-slip point double couple vary continuously as the source is moved across the boundary (see equations 66 and 67 or Figure 4), when we integrate the double couples over a finite

Point Sources as They Cross a Boundary

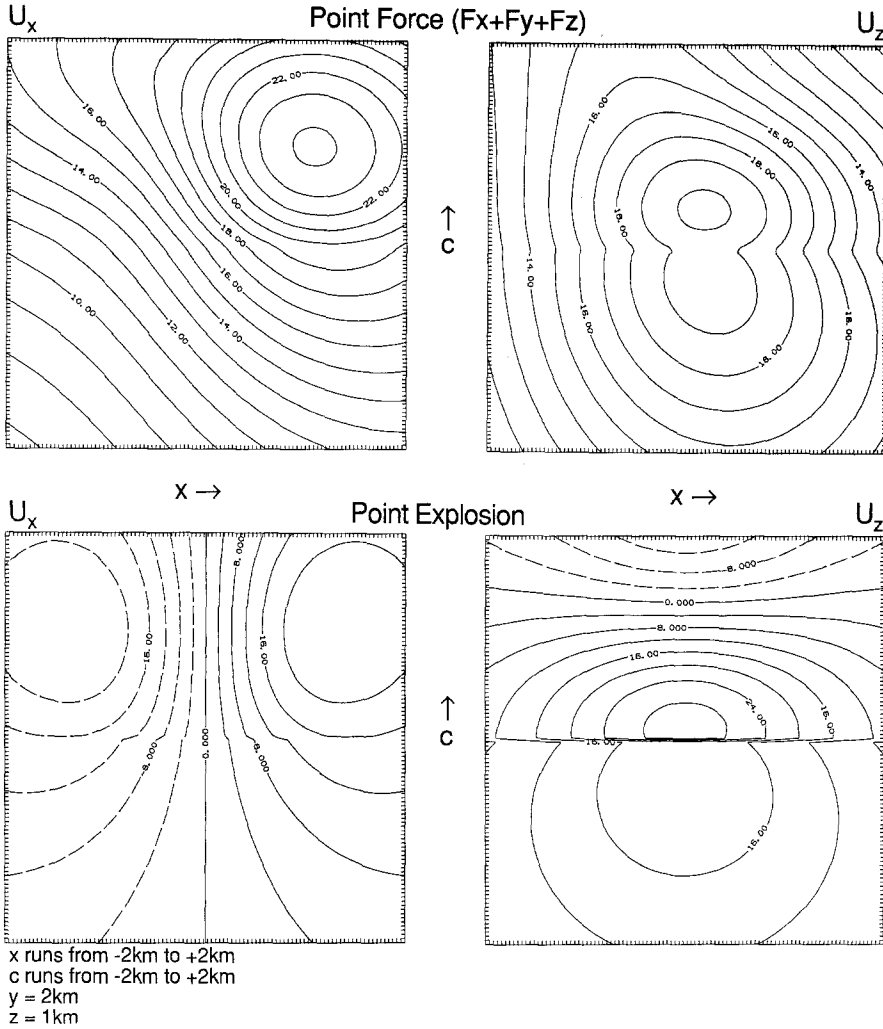


FIG. 7. Same as Figure 4, but for a point-force ($F_x = F_y = F_z = 10^{19}$ dyne) and for a point explosion ($M_0 = 10^{25}$ dyne-cm). Notice that the deformation from any point force varies continuously as the source crosses the interface, but the pattern of the deformation from a point explosion jumps as the source crosses the interface.

plane, then the displacements produced at that plane jump by a ratio of the rigidities as the source plane crosses the boundary. This type of behavior was already discussed immediately after equation (68).

In Figure 9, we show the deformations that result from horizontally oriented double couples (0° dip) distributed on horizontally oriented fault planes located just 0.01 km above the material interface (panels 9a and 9b) and 0.01 km below the interface (panels 9c and 9d). As before, the rigidities of the upper and lower media are 1.0×10^{11} and 2.0×10^{11} dyne/cm², the fault is 4 km by 4 km and the total moment is 10^{25} dyne-cm. The observer grid for panels 9a and 9c is located 0.1 km above the interface and parallel to the source plane; the observer grid runs along the x axis from -3 km to $+3$ km and along the y axis from -3 km to $+3$ km. In

Displacement Parallel to Slip; Finite Faults (4km x 4km)
Perpendicular to Boundary and with Uniform Moment

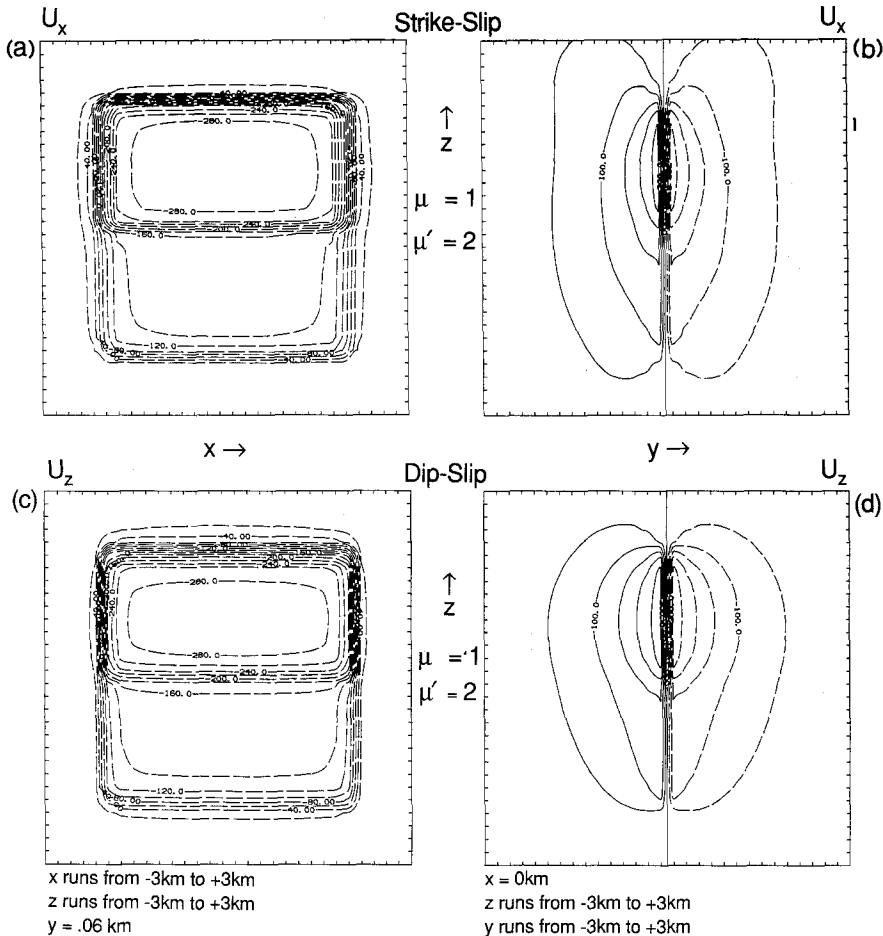


FIG. 8. Displacements parallel to the slip direction for numerical integration of double couples over vertically dipping planes of length 4 km and width 4 km. Upper panels are for strike-slip double couples and lower panels are for dip-slip double couples. The moments are evenly distributed over the fault planes and the total moment is 10^{26} dyne-cm. The fault planes intersect an interface between a material of rigidity of 10^{11} dyne-cm⁻² and another material of rigidity 2×10^{11} dyne-cm⁻². In the left panels, the displacements are contoured on a plane that is parallel to and 0.06 km from the source plane. In the right panels, the displacements are contoured on a vertical plane that is perpendicular to the source plane (intersecting its middle). In both cases, the summation of double couples mimics slip on a finite fault where the slip is inversely proportional to the rigidity of the surrounding medium.

panels 9b and 9d, the observer grid is perpendicular to the source plane and runs along the x axis from -3 km to $+3$ km and along the z axis from -3 km to $+3$ km. The deformations produced by these distributions of double couples mimic dislocations along the source planes, and in both cases, the upper medium experiences displacements that are twice as large as in the lower, more rigid medium. The jump in displacement across the source plane is twice as large for the source located slightly above the interface (panels 9a and 9b) as the jump in displacement for the source located just below the source plane. This is in agreement with the notion that $D = M_0/\mu A$, where μ is the rigidity of the medium in which the dislocation is located. We see that the pattern of displacements produced by the source located just below the plane is virtually identical (but smaller in magnitude by a factor of

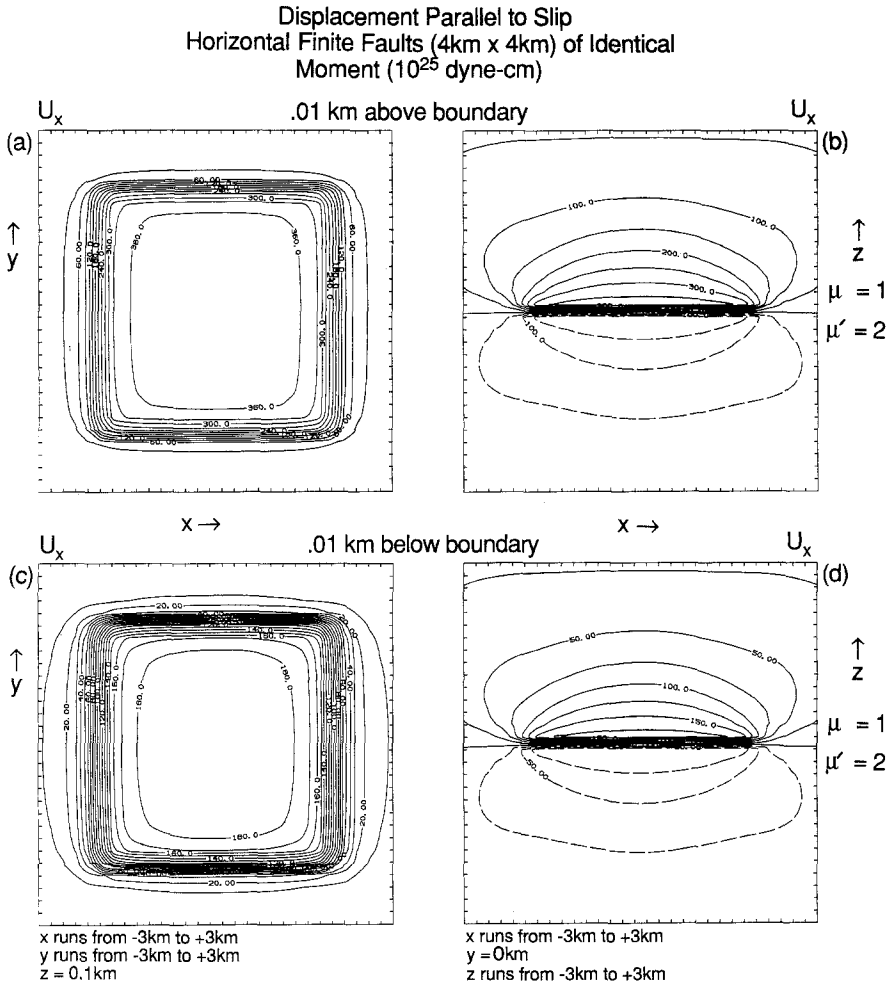


FIG. 9. Displacements parallel to the slip direction for numerical integration of horizontal double couples over horizontal planes of length 4 km and width 4 km. In the upper panels, the horizontal fault plane is located 0.01 km above an interface between rigidities of 10^{11} and 2×10^{11} dyne-cm $^{-2}$, and in the lower panels, the horizontal fault is located 0.01 km below the interface. In both cases, the total moment of the finite source is 10^{25} dyne-cm. In the left panels, the displacements are contoured on a horizontal plane that is parallel to the fault planes and that is 0.1 km above the interface. In the right panels, the displacements are contoured on a vertical plane that bisects the fault plane in its middle along its slip direction. The deformation from the summation of double couples mimics slip on a horizontal fault. Notice that the slip is twice as large on the upper side of the source (panels b and d) and that the deformations for the source located just above the interface (panels a and b) are twice as large as the deformations for the source located just below the interface (panels c and d). The deformations from a horizontal source located just above the interface would be identical to those produced by a source with twice the moment but located just below the interface. In this example, we see that the moment of a dislocation on a fault separating different materials is ambiguously defined.

2) to that produced by the source with the same moment that is located just above the interface. If we assumed that the moment of the finite source in the lower medium was twice the moment of the similar source in the upper medium, then the two sources would produce virtually identical patterns of deformation everywhere in the medium. Although these sources would be virtually indistinguishable, they would have dramatically different seismic moments.

DISCUSSION AND CONCLUSIONS

We have produced analytic expressions for the static deformations caused by point force and force-couple systems embedded in two welded Poissonian half-

spaces. These expressions allow us to verify that the deformation in the limiting vicinity of the source is independent of the material properties of the half-space without the source. Of course, this result is not new since it has already been proven in a more general way (Aki and Richards, 1980; equation 3.5). We have also shown that the way in which the deformation changes as a point source is moved across a material interface is complex. The deformations produced by point forces or by vertical strike-slip point double couples vary continuously (except in the limiting vicinity of the strike-slip source) as the source is moved across a boundary. As a vertical (or horizontal) dip-slip double couple is moved across a boundary, the deformation pattern varies continuously but the amplitudes jump by the ratio of the rigidities. If the source is either a point explosion or a point double couple dipping at some angle other than 0° or 90° , then the deformation pattern jumps as the source is moved across the boundary. Inversion of data for the moment tensor of a point source in the vicinity of a boundary can lead to different orientations (and spurious non-double-couple components) for the source depending upon whether the source is assumed to lie above or below the boundary.

We have shown that numerical integration of point double couples over a finite planar surface produces a deformation pattern that mimics a dislocation on that surface and that as expected, the dislocation is given by $D = M_0/\mu A$, regardless of the orientation of the source and the proximity to the boundary. Furthermore, integration of double couples over horizontally dipping finite faults located just above and below a material interface may produce identical deformations even though the total moments of the sources differ by the ratio of the material rigidities.

In a way, none of these conclusions should come as a surprise. However, there are some conceptual problems that result when we interpret these results in the context of the moment tensor of an earthquake. The size of an earthquake is often given in terms of its moment. Yet we have just seen that there are cases in which virtually indistinguishable elastic deformations (even in the vicinity of the source) can be produced by sources having significantly different total moments (just move a horizontally dipping source an infinitesimal distance across a material interface). Just what is the moment of an earthquake when the two sides of the fault have different rigidities? At least two (and perhaps another) perfectly acceptable numbers can be given. Assume the double couples are infinitesimally close to either side of the boundary, or perhaps assume that the double couples actually straddle the boundary (a problem that we have not solved here). In fact, the same deformation would result if we assume that some fraction of the total slip D is modeled by a source just above the interface and the rest of the slip is modeled by a source just below the interface. In this case the moment could be any number between μAD and $\mu'AD$ (Woodhouse, 1981).

This apparent paradox can be better understood by reviewing just what it is we mean when we assign an earthquake a moment. Certainly it seems a little odd to describe the overall size of an earthquake (actually slip on a fault plane) with a torque. The moment that we assign to an earthquake is the total moment of a distribution of point double-couple body forces that, when applied to the medium, produces the same pattern of deformation as slip on some fault plane. Unfortunately, there are cases where the same pattern of deformations can be produced by very different distributions of double couples.

If we wish to describe some overall magnitude of the slip on the fault plane, then why not simply integrate the dislocation over the rupture surface? Ben-Menahem and Singh (1981, equation 4.94) call this parameter *potency* and they use it as a basic source scaling parameter. If either the dislocation or the area of a very small

source were to double, then the resulting deformation would double throughout the medium. However, if the rigidity is assumed to change in the region of a given dislocation, then the deformation does not necessarily change in a corresponding fashion. If we assume a fixed moment and we allow the rigidity to become very large, then the resulting deformations would become vanishingly small and so would the radiated energy and the change in strain energy. In fact, if we explicitly substitute μAD for M_0 into all of the solutions given in this paper, then the μ would trivially cancel and the properties of the media would only enter into the solutions through the ratio of the rigidities m ! In this case, the fundamental source scaling parameter is potency as defined by Ben-Menahem and Singh (1981).

A similar argument can be made in the case of the waves radiated from a dislocation that is simulated with double couples. In virtually all equations that express the far-field displacements resulting from double-couples having a moment M_0 , there is a scaling factor $M_0 \rho^{-1} v^{-3}$, where ρ is the density and v is some wave velocity intrinsic to the medium. In all of these cases, this factor can be reduced to the factor $AD(\eta v)^{-1}$, where η is a dimensionless material constant that depends on Poisson's ratio ν ($\eta = 1$ if v is the shear-wave velocity and $\eta = \frac{2 - 2\nu}{1 - 2\nu}$ if v is the compressional-wave velocity). The remaining inverse velocity term can be intuitively interpreted as a term that relates the size of the displacements that occur in the source region to the size of waves that are radiated to the far field. That is, it gives the relative importance of inertial forces (related to ρ) to the elastic restoring forces in a medium (related to η and μ). We see, then, that there is a superfluous $\rho^{-1} v^{-2}$ term that is introduced just to cancel the superfluous μ that crops up when we scale with seismic moment.

As another example, suppose that a rupture with area A and dislocation D occurs within a thin layer of low rigidity that is sandwiched between two high-rigidity half-spaces (for example, a low rigidity zone of fault gouge). What is its seismic moment? Which rigidity should be use? Of course, the answer is that we should use the rigidity of the material in which the source is embedded, the low-rigidity material. However, this seems rather counter-intuitive since most of the deformation occurs in the material surrounding this thin zone. Certainly, the fact that there are high rigidities surrounding the rupture should tell us something about the size of the earthquake. A little thought tells us that we would actually get about the same deformation and change in strain energy if we forgot about the low-rigidity material and just modeled the rupture in a homogeneous whole-space. However, we would obtain a different seismic moment for these two models, even though the changes in strain energies were approximately the same and the potencies were identical. This is just another example of why seismic moment is not a very satisfying way to describe the size of an earthquake.

If one wishes to calculate the change in strain energy (an excellent candidate for the description of the overall size of an earthquake) produced by a distribution of double couples, then one must completely describe the properties of the medium (including the state of prestress) as well as the exact locations in which those body forces are applied. In other words, the seismic moment is not a very satisfying measure of the size of an earthquake unless the complete description of the properties of the medium and the way in which those moments were applied is also given.

Although change in strain energy or perhaps total radiated energy (not necessarily the same quantities) may be more satisfying measures of the overall size of an

earthquake, they are also much more difficult to calculate. This is particularly true of change in strain energy since it requires knowledge of the ambient stress level as well as a model that does not contain non-integrable strain-energy singularities such as occur at the edges of faults with uniform dislocations. Potency (AD) is relatively easy to estimate and it is an obvious choice for a size-scaling parameter, having none of the ambiguities associated with seismic moment. However, as long as the range of rigidities encountered in seismogenic regions does not vary too wildly, seismic moment does provide some overall sense of the size of an earthquake. Certainly it has many advantages over other traditional magnitude scales. Furthermore, when the entire model is precisely specified, the distribution of point-force systems does provide a complete description of the seismic source. Thus, seismic moment will continue to be a convenient and useful parameterization of earthquakes. However, when using this parameterization, it is also important to understand the origin of the concept and its inherent limitations and potential ambiguities.

ACKNOWLEDGMENTS

We thank Jim Knowles for leading us to Rongved's paper and we thank Jim Rice for providing an unpublished manuscript having an alternative derivation of the solution for point forces in two welded half-spaces. Both of these papers provided valuable insight into this problem. We also thank Hiroo Kanamori for enlightening discussions. We thank Jim Savage, Joe Andrews, and Terry Wallace for their reviews.

REFERENCES

- Aki, K. and P. G. Richards (1980). *Quantitative Seismology*, vol. 1, W. H. Freeman, San Francisco, 557 pp.
- Ben-Menahem, A. and A. Gillon (1970). Crustal deformation by earthquakes and explosions, *Bull. Seism. Soc. Am.* **60**, 193-215.
- Ben-Menahem, A. and S. J. Singh (1981). *Seismic Waves and Sources*, Springer-Verlag, New York, 1108 pp.
- Fung, Y. C. (1965). *Foundations of Solid Mechanics*, Prentice-Hall International, London, 525 pp.
- Haskell, N. A. (1964). Total energy and energy spectral density of elastic wave radiation from propagating faults, *Bull. Seism. Soc. Am.* **54**, 1811-1841.
- Mansinha, L. and D. E. Smylie (1971). The displacement fields of inclined faults, *Bull. Seism. Soc. Am.* **61**, 1433-1440.
- Rongved, L. (1955). Force interior to one of two joined semi-infinite solids, *Proc. of the 2nd Midwestern Conference on Solid Mechanics*, J. L. Bogdanoff (Editor), Research Series No. 129, Engineering Experiment Station, Purdue Univ., Indiana, 1-13.
- Sato, R. (1971). Crustal deformation due to dislocation in a multi-layered medium, *J. Phys. Earth* **19**, 31-46.
- Sato, R. and M. Matsu'ura (1973). Static deformations due to the fault spreading over several layers in a multi-layered medium Part I: Displacement, *J. Phys. Earth* **21**, 227-249.
- Woodhouse, J. H. (1981). The excitation of long period seismic waves by a source spanning a structural discontinuity, *Geophys. Res. Lett.* **8**, 1129-1131.

U. S. GEOLOGICAL SURVEY
525 S. WILSON AVENUE
PASADENA, CALIFORNIA 91106
(T.H.H.)

EMERITUS, RUTGERS UNIVERSITY
NEW BRUNSWICK, NEW JERSEY
(R.E.H.)

Manuscript received 27 July 1988